ABSTRACT

It is well known that, when accelerated electrons from a linear accelerator interact with a high atomic number (Z) target material, electromagnetic radiation (bremsstrahlung) is produced. In the present work some aspects of the generation of the bremsstrahlung radiation by linear accelerators of electrons are studied, namely the relation between the dose and parameters of the accelerating structure and beam characteristics is investigated. We carry out numerical simulations of the relative dose rate at fixed maximal beam energy and analyze its dependence on the length of the accelerating cells, power of the electromagnetic field dissipated in them and average energy and energy spread of the output beam. The simulation of the acceleration of the electrons in the accelerator is done with the RTMTRACE code.

RESUMEN

Como es bien sabido, cuando electrones acelerados en un acelerador lineal interaccionan con un blanco de un material con elevado número atómico (Z), se produce radiación electromagnética (bremsstrahlung). En el presente trabajo se estudian algunos aspectos de la generación de bremsstrahlung con aceleradores lineales de electrones, por ejemplo se investiga la relación entre la dosis y parámetros de la estructura de aceleración y entre dosis y características del haz. Se han llevado a cabo simulaciones numéricas de la dosis relativa a una energía máxima del haz fija y se ha analizado su dependencia de la longitud de las celdas de aceleración, potencia del campo electromagnético disipada en ellas y energía media y dispersión energética del haz de salida. La simulación de la aceleración de los electrones en el acelerador se hace con el código RTMTRACE.

CONTENTS

ABSTRACT/RESUMEN 1
1) INTRODUCTION 5
2) DEFINITIONS 9
3) DESCRIPTION OF THE EXPERIMENTAL FACILITY SIMULATED 15
4) COMPUTATIONAL PROCEDURE 17
5) DOSE RATE STUDY 21
5.1) Relative dose rate 21
5.2) Dependence of dose rate on energy spread 22
6) NUMERICAL SIMULATION OF THE ELECTRON ACCELERATION 27
6.1) Maximal output energy 27
6.2) Calculation of the output beam spectrum and the relative dose rate 34
7) ANALYSIS OF THE RESULTS 37
7.1) Beam acceleration 39
7.2) Dose production 44
8) ECONOMIC AND ENVIRONMENTAL ANALYSIS 49
8.1) Economic analysis 49
8.2) Environmental analysis 49
9) CONCLUSIONS 51
ACKNOWLEDGEMENTS 53
REFERENCES 55
APPENDICES 57
A) DoseCalc FORTRAN code 57
B) Results 73
B.1) Maximal output energy. 73
B.2) Relative dose rate. 75
B.3) Energy spectra 78
C) Analysis of the energy spectrum width 81
D) Budget 85

1) INTRODUCTION

When charged particles with energies large compared to their rest energies (relativistic particles) are decelerated over a very short distance (i.e. in a target material), the bremsstrahlung electromagnetic radiation is produced. Since electrons are much lighter than protons, electron bremsstrahlung is the most common. The intensity of electromagnetic radiation depends upon the energy and current of the incident electrons, the atomic number and thickness of the target material, and the angle between the direction of observation and the incident electron beam. Generally, the use of targets with high atomic number, such as Lead, Gold or Tungsten, enhances the bremsstrahlung yield. In addition, the yield increases with the electron energy [1][2][3][4].

Due to the penetrating properties of bremsstrahlung and its effects on materials and biological organisms, this radiation can be used for different purposes in industrial radiation processing, medicine, elemental analysis, safety systems, defectoscopy, etc.

Radiation processing has been widely accepted for use in many areas of the global economy. Sterilization, polymer cross-linking (tapes, tubes, and cables), tire component curing, the conservation of art objects and the irradiation of selected food items are well established technologies. They are yielding tremendous industrial and social benefits in the fields of material science, healthcare, food and environment. For example, radiation induced polymerization and polymer modifications, namely surface curing, crosslinking and degradation brought out value addition to the products through an environment-friendly, economically beneficial process and has emerged as a multimillion dollar industry. Presently, processing of materials using high energy electron accelerators (200 keV to 10 MeV) constitutes the largest commercial radiation application. World over, there are more than 1000 accelerators operating in the wire/cable, heat shrinkable tubing, surface curing and other related industries. Radiation processed polymers possess superior mechanical, electrical and thermal stability compared to conventionally crosslinked ones. The process is simple and can be controlled by only one single parameter, namely the absorbed dose, quantity that varies with the application as indicated in Table 1.1 [5].

Table 1.1. Some radiation processing applications and the absorbed dose required.

Application	Dose Required [kGy]
Disinfection	0,25 to 1
Food preservation	1 to 25
Medical Sterilization	20 to 30
Curing of coatings	20 to 50
Polymerisation	50 to 100
Crosslinking of polymers	100-300
Coloration of Diamonds	>>>2000

Many gamma ray irradiators have been built and it is estimated that about 200 are currently in operation in member States of the International Atomic Energy Agency (IAEA). Gamma ray emitters like cobalt-60 became popular radiation sources for medical and industrial applications. In recent times, the use of electron accelerators as a radiation source (and sometimes equipped with X ray converter) is increasing [6]. This increase is mainly due to two advantages, first with accelerators the production of radiation can be controlled with an on-off switch, allowing more safe and easy operation; and second, the accelerators can also directly irradiate the target with the electron beam.

The first charged particle accelerator has been constructed nearly 90 years ago. The fast growth of accelerator development was connected to the rapid growth of nuclear experimental studies at that time. Cascade generator, electrostatic accelerator, linear accelerator (linac) and cyclotron were constructed in a short period of time at the beginning of thirties. The main differences between those accelerators were based on differences in electric field generation and the accelerated particles trajectory shape. The primary accelerator application was strictly related to the field of nuclear physics. The fast development of accelerator technology created the opportunity to increase the field of application towards chemistry, medicine and industry. New ideas for accelerator construction and progress in technical development of electrical components were the most importance factors in process of accelerator technology perfection [7].

Table 1.2. Accelerators in the world updated for EPAC2000 [8].

Category	Number
Ion implanters and surface modification	7000
Accelerators in industry	1500
Accelerators in non-nuclear research	1000
Radiotherapy	5000
Medical isotopes production	200
Hadrontherapy	20
Synchrotron radiation sources	70
Research in nuclear and particle physics	110
TOTAL	**15000**

As it is showed in Table 1.2 there are approximately 15000 accelerators over the world and most of them are used for commercial applications, approximately half for medical treatment and half for industrial applications. Medical accelerators treat cancer and other diseases of millions of people each year, while industrial accelerators are used for processing numerous products with charged particle beams and for doing analysis on many others. Industrial accelerators include all accelerators that generate external beams for use in beam processing other than medical treatment or physics research. Those devices that use low energy charged particles internally, such as cathode ray tubes, x-ray tubes, radio frequency and microwave tubes and electron microscopes, are not included [9].

Electron linear accelerators (linacs) in the energy range from 1 to 16 MeV are widely used for non-destructive inspection applications. Penetrating high energy x-rays generated by bombarding a tungsten target have been used for almost 50 years to locate flaws in large metal castings and welded joints as well as to inspect large solid-fuel rocket motors. Because the parts being inspected are often very large and heavy, early commercial units were designed to be mobile so they could be moved around the part. With the advent of real-time detection technology, high energy x-ray inspection systems were developed. Also, the in-situ inspection of parts in fixed installations, such as parts of nuclear power plants and bridges, required the development of very compact portable systems. A newer, much larger application of high energy electron linacs is the inspection of large cargo containers and semi-trailers at border entry points. Originally deployed to stop the entry of weapons and illicit materials, these systems are now also being used for cargo inspection as showed in Figure 1.1 [9].

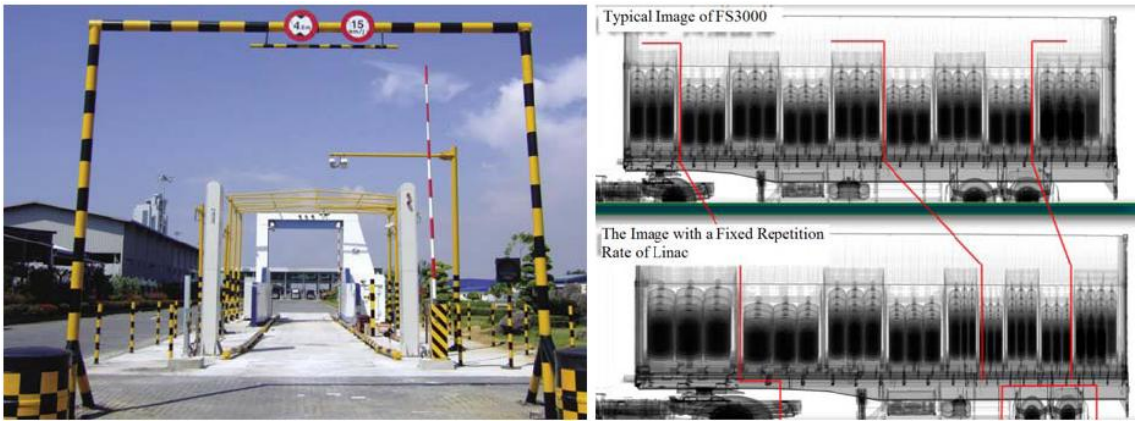

Figure 1.1. Fast scan cargo inspection system (left) and its typical image (right) [10].

The goal of the present work is to study, through numerical simulations, the dose rate of the generated radiation and its dependence, at fixed maximum energy in the beam, on the main linac parameters, such as length of the accelerating cavities and dissipated power of the accelerating electromagnetic field in them, and beam parameters, such as the average energy and the energy spread. The simulation of the acceleration of the electrons in the accelerator is done with the RTMTRACE code created at the Moscow State University. In this work, no simulation of the bremsstrahlung production is done and the dose rate is estimated using an empirical formula taken from the literature. Also the target characteristics, such as material and thickness, are pre-determined and supposed to be optimal; the dose rate dependence of them is beyond the scope of this work.

The present work has a relation to a 12 MeV Race-Track Microtron (RTM) project of the UPC [11] which consists in building a compact electron RTM for medical applications. It is carried out by a collaboration of the UPC, several Spanish centres and companies and Skobeltsyn Institute of Nuclear Physics of Moscow State University. The type of the accelerating structure considered in our study is the same as that of the 12 MeV RTM. In this sense our results and conclusions may be of some use for the optimization of the electron acceleration in the RTM.

Having obtained results of the beam simulations and dose calculations we analyze this data and find optimal linac parameters for which the generated dose rate is maximal.

2) DEFINITIONS

We begin with giving some basic definitions of concepts and notions related to accelerators.

Rf Linac (Radio Frequency Linear Accelerator): Resonant linear accelerators (Figure 2.1) are usually single-pass machines. Charged particles traverse each section only once; therefore, the kinetic energy of the beam is limited by the length of the accelerator. There are two types of electron RF linacs – standing wave and travelling wave. For standing wave type the operation of accelerator is based on electromagnetic oscillations in tuned coupled structures (resonant cavities). In travelling wave RF linac diaphragms installed in circular waveguide slow down a travelling wave with longitudinal electric field component so that its phase velocity is close to the velocity of accelerated particles [13].

Figure 2.1. 9 MeV standing wave electron linac for industrial applications [10].

Resonant Cavity: A resonant cavity (Figure 2.2) is a volume enclosed by metal walls that supports an electromagnetic wave oscillation. In accelerator applications, the oscillating longitudinal electric field accelerates charged particles while the oscillating magnetic fields provide inductive isolation [13].

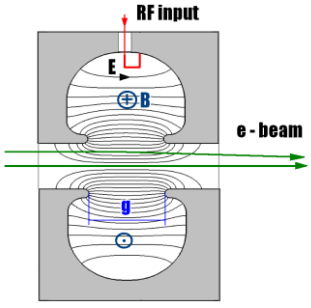

Figure 2.2. Axial section of a resonant cavity. Directions of the electric (E) and magnetic field (B) are shown.

Accelerating structure: An accelerating structure consists of one or more resonant cavities. Depending on the phase shift of the electric field per cavity there are different types of accelerating structures as showed in Figure 2.3. For example, in the π-type accelerating structure the electric field changes in each neighbouring cavity and in the $\frac{\pi}{2}$-type the change is every two neighbouring cavities.

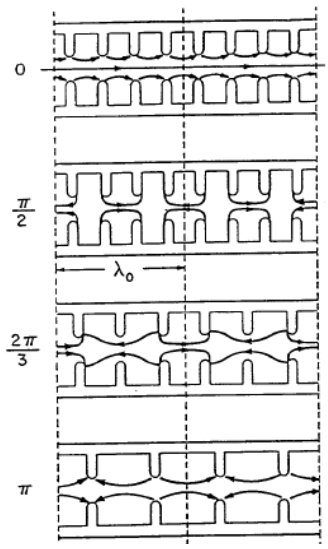

Figure 2.3. Field configurations with different phase shift per cell.

Parameter* β*: In the theory of relativity the parameter β is defined as the ratio of the particle speed v to the speed of light c.

$$\beta = {}^{v}/_{c} < 1 \qquad \text{(Eq. 2.1)}$$

In π-type accelerating structures the cell length L must be such that a particle with velocity $v = \beta c$ passes it during half RF period T_{RF}.

$$L = \frac{1}{2} v \cdot T_{RF} = \frac{1}{2} \beta \cdot \lambda \qquad \text{(Eq. 2.2)}$$

where λ is the RF wave length. In this *synchronism condition*, the parameter β is a dimensionless number characterizing the cavity length.

Particle phase: The electric field in the longitudinal direction at the centre of the cavity $\mathcal{E}_z$ varies in time as:

$$\mathcal{E}_z = \mathcal{E}_{max} \cos(\omega_{RF} \cdot t) = \mathcal{E}_{max} \cos(2\pi f_{RF} \cdot t) \qquad \text{(Eq. 2.3)}$$

where $\mathcal{E}_{max}$ is the amplitude of the electric field in the cavity axis, $\omega_{RF} = 2\pi f_{RF}$ and f_{RF} is the

frequency of the RF wave, see Figure 2.4.

If we assume that a particle, with velocity v, enters in the cavity at a given time t_0, then the distance z covered by the particle in the cavity is:

$$z = v \cdot (t - t_0) \quad \text{(Eq. 2.4)}$$

Then, if we define the phase as $\varphi = \omega_{RF} \cdot t = 2\pi f_{RF} \cdot t$, we can obtain an expression of the distance covered by the particle in the cavity as a function of the phase:

$$z = \frac{v}{\omega_{RF}} \cdot (\varphi - \varphi_0) = \frac{v}{2\pi f_{RF}} \cdot (\varphi - \varphi_0) \quad \text{(Eq. 2.5)}$$

where φ_0 is the initial phase at time t_0.

Therefore the particle phase is a parameter which refers to the position of the particle at a certain moment in time and relates it to the electric field level. A *synchronous particle* is defined as a particle that has the same phase in all cavities, the *synchronous phase*. The synchronous particle is in longitudinal equilibrium. Acceleration of the particle in the cavities matches the phase difference of electromagnetic oscillations between cavities so that the particle always crosses gaps at the same relative position in the waveform.

In general, the change in the particle velocity is small during passage of one rf-cavity and the kinetic energy gain is maximal when the field reaches the maximum at the moment the particle is in the middle of the cavity. The accelerating cavity voltage is defined

$$V_{RF} = \int_{-L/2}^{L/2} \mathcal{E}_{max}(z) \cos\left(\frac{2\pi z}{\beta\lambda}\right) dz \quad \text{(Eq. 2.6)}$$

If the electric field amplitude is constant within cavity length Eq. 2.6 leads to

$$V_{RF} = L \cdot \mathcal{E}_{max} \cdot T \quad \text{(Eq. 2.7)}$$

And therefore, the kinetic energy gain is after integration of the time-dependent field along the particle path

$$\Delta E_{kin} = |e| \cdot L \cdot \mathcal{E}_{max} \cdot T \quad \text{(Eq. 2.8)}$$

where we have defined the transit-time factor

$$T = \frac{\sin\frac{L\cdot\omega_{RF}}{2v}}{\frac{L\cdot\omega_{RF}}{2v}} \qquad \text{(Eq. 2.8)}$$

The transit-time factor gives the correction on the particle acceleration due to the time variation of the field while the particles traverse the cavity [12].

Figure 2.4 defines the phase of a particle with respect to a travelling wave, in particular the synchronous phase φ_s. For electron acceleration, the wave accelerates particles when the electric field is negative[13][14].

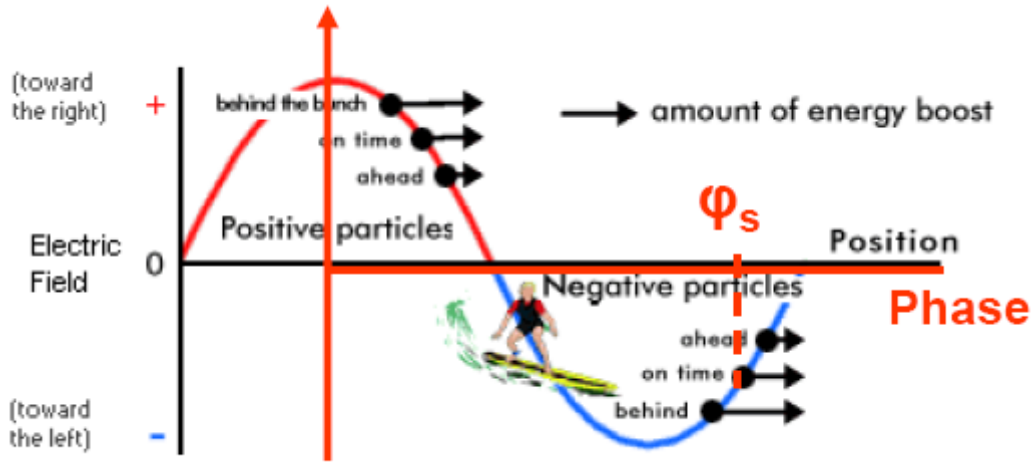

Figure 2.4. Axial variation of the longitudinal electric field of a travelling wave at a given time.

Power dissipated in a cavity: The power dissipated in the cavity walls P_w due to induced currents is related to particle acceleration. The wall losses are often expressed in terms of the total voltage or the electrical field defined (supposing, again, that the electric field amplitude is constant within cavity length) as

$$P_w = \frac{\mathcal{E}_{max}{}^2}{r_s} \qquad \text{(Eq. 2.9)}$$

where $r_s$is the shunt impedance per unit length [12].

Thus, we can set the electric field level using the dissipated power as a parameter.

Dose: The notion of dose refers to the amount of energy absorbed by an object or person per unit mass. Depending on its definition different types of dose may be distinguished as shows Table 2.1 [15][16][17].

Table 2.1. Summary of important radiation protection quantities and units.

	Types of radiation for which it is defined	Type of media in which it is defined	Example of generic units	Example of special units
Exposure (X)	X and gamma rays	Air	C/kg	R(roentgen) = $2.58 \cdot 10^{-4}$ C/kg
Absorbed Dose (D)	All	Any	Gy (gray) = 1 J/kg	1 rad = 100 erg/g = 0.001 Gy
Equivalent Dose (H)	All	Human Tissue	Sv (Sievert) = $w_R \cdot 1$ J/kg	1 rem = $w_R \cdot 100$ erg/g = $w_R \cdot 0.001$ J/kg

The absorbed dose D is defined as the mean energy dE transmitted by ionizing radiation to the mass dm of density ρ in the volume dV:

$$D = \frac{dE}{dm} = \frac{dE}{\rho \cdot dV} \qquad \text{(Eq. 2.10)}$$

Exposure X is defined as the sum of the electrical charges dQ of all the ions of one sign produced in air by X-rays or gamma radiation when all electrons liberated by photons in a suitably small element of volume dV of air are completely stopped in air, divided by the mass dm of air in the volume element.

$$X = \frac{dQ}{dm} = \frac{dQ}{\rho \cdot dV} \qquad \text{(Eq. 2.11)}$$

A simple analysis can show that the exposure in air can be related to the dose delivered, by photons, to air. Assume that a source is giving off radiation such that 1 roentgen (1 R) is measured in a given time period. Knowing the definition of a roentgen, and that any ion pair carries 1.6×10^{-19} C of charge of either sign, and furthermore that it takes about 34 eV of energy to create one ion pair in air, we can write:

$$1\ R = 2.58 \frac{C}{kg} \cdot \frac{1\ ion}{1{,}6 \cdot 10^{-19}\ C} \cdot \frac{34\ eV}{ion} \cdot \frac{1{,}6 \cdot 10^{-19}\ J}{eV} \cdot \frac{1\ Gy}{1\ {}^{J}/_{kg}} = 0.00877\ Gy = 0.877\ rad$$

To take into account the biological effects of different kinds of radiation, radiation weighting factors w_R were introduced by the International Commission on Radiological Protection (ICRP) in 1990

(Table 2.2). The weighting factor w_R indicates the ratio of the degree of a certain biological effect caused by the radiation considered, to that caused by X rays or γ rays at the same energy absorption. It is laid down on the basis of the experience gained in radiation biology and radiology.

The equivalent dose H is measured in sievert (Sv) and defined as

$$H = w_R \cdot D \qquad \text{(Eq. 2.12)}$$

where D is the absorbed energy dose, measured in Gy.

Table 2.2. Radiation weighting factors.

Type of radiation	Weighting factor w_R
Photons (X and y rays)	1
Electrons and muons	1
Neutrons, energy:	
<10 keV	5
10 keV to 100 keV	10
>100 keV to 2 MeV	20
>2 MeV to 20 MeV	10
>20 MeV	5
Protons, other than recoil protons, E>2MeV	5
Alpha particles, fission fragments, heavy nuclei	20

3) DESCRIPTION OF THE EXPERIMENTAL FACILITY SIMULATED

In the present study some settings of the installation simulated are supposed to be fixed, others are optimized by simulations with the RTMTRACE code to obtain the desired output properties.
Figure 3.1 gives a detailed view of the axial section of the accelerating structure [18] (note that in this image the beam enters from the right hand side of the accelerating structure).

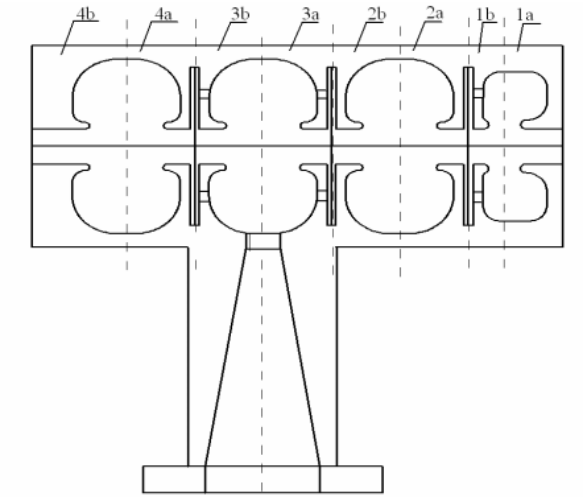

Figure 3.1. Axial section of the accelerating structure.

The main linac characteristics and input beam properties are the same as those of the accelerating structure used in the RTM under construction in UPC.

The linac is composed by one cavity with $\beta=\beta_1$ which will be varied between 0.5 and 1 and three cavities of $\beta=\beta_2=1$. The first cavity is shorter than the other three because the linac must effectively accelerate a non-relativistic beam from the electron gun.

As summarized in Table 3.1, the energy gain per passage is set to $\Delta E_s = 2MeV$ with a synchronous phase of $\varphi_s = 16º$, due to the relation $\Delta E_s = \Delta E_{max} \cos(\varphi_s + \pi)$ (note that π is added to the synchronous phase to take into account that electrons are accelerated by negative voltages), the maximum energy gain is $\Delta E_{max} = 2.08MeV$. The working frequency is set to $F = 5712MHz$.

Table 3.1. Linac characteristics.

LINAC	
Maximum energy gain [MeV]	2.08
Frequency of the RF source [MHz]	5712
Number of cavities with β<1	1
Number of cavities with β=1	3
Dissipated RF power	Optimized to obtain desired energy gain

The injected beam is supposed to be circular, monoenergetic and continuous. Its characteristics are summarized in Table 3.2.

Table 3.2. Input beam properties.

INJECTED BEAM	
Type	Circular beam
Diameter[mm]	1
Kinetic Energy [keV]	25
Initial phase (PHI) [º]	-180<PHI<180

The complete experimental facility, which is simulated in the present study, is composed by the linac, a bremsstrahlung target placed at the exit of the linac to produce the electromagnetic radiation and a detector placed at 1 m from the target. We would like to remark that, in the present study, only the acceleration of the electrons in the linac is simulated and the dose rate is estimated with an empirical formula taken from the literature. Therefore, the target characteristic will not enter in the study, for example the effects of the target thickness, typically about 1-2 mm, on the dose rate are not studied. Figure 3.2 shows a simplified view of the whole installation (note that the picture is not of proper scale).

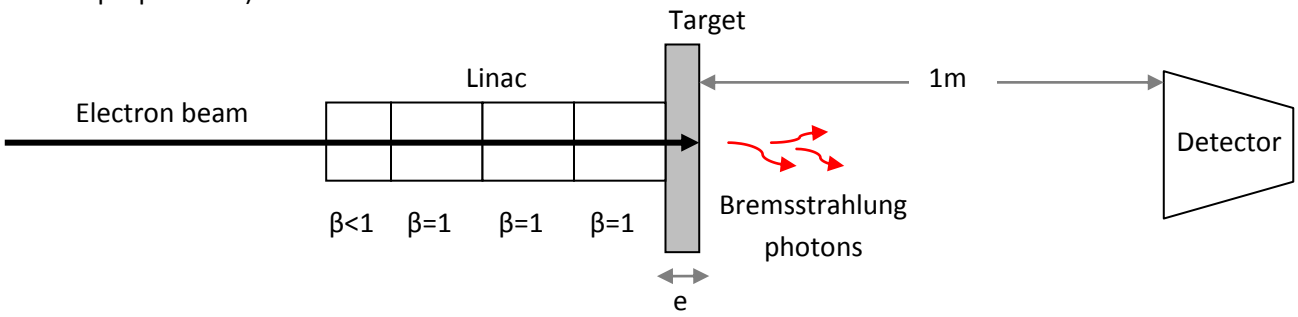

Figure 3.2. Simplified scheme of the simulated installation.

4) COMPUTATIONAL PROCEDURE

The simulations of the electron acceleration were done using the RTMTRACE code [19] developed at the Skobeltsyn Institute of Nuclear Physics of Moscow State University.

The main part of the RTMTRACE code is designed for simulations of the beam dynamics in the race-track microtron and its main systems: chopper, buncher, capture section, linear accelerator, beam transport lines, 180 deg. end magnets etc. However, in this study only the linear accelerator is simulated.

RTMTRACE code makes it possible to investigate behaviour of individual particles with their initial 6-D coordinates defined by user, as well as of the ensemble of particles distributed randomly within given boundaries in 6-D hyper-space. Input data for the code consist of a sequence of commands, and of additional files, which are not used in the present study because these files are not needed for the linac simulation. Each command with its parameters must be placed at separate card (string) and the first card must be the card describing the beam. All commands are contained in the input file with the name **inp.dat.**

Results of calculations, depending on the command used and their parameters are directed into the file **out.dat** , to computer monitor (phase diagrams) or to other additional files.
The main commands with some of the subsequent subcommands used in the present work are described in Table 4.1

Table 4.1. Main RTMTRACE commands and subcommands used in this work.

COMMAND	FUNCTION	SUBCOMAND	FUNCTION
BEAM	Input of the beam parameters	**IST=4** **IST=5**	Individual particles start Circular beam with normal random distribution
DATAL	Data input for the linac	**NTYP=1**	Integration of 6 equations in the field, given by the cos decomposition of the measured or experimental on-axis field.
INTL	Integration for the linac	**IGRA=1**	For IST=4, displays dependence energy-initial phase (E-PHI)
DUMP	Save particle vectors in *dump.dat*	**NDUMP**	Number of the dump to be done
GRAF	Display phase diagrams	**IXXP=1** **IYYP=1** **IPDE=1** **IXY=1**	X-XP phase space projection Y-YP phase space projection PHI-DE phase space projection Beam spot

Table 4.2 gives a further description of the main code parameters for the beam and the linac simulation setup.

Table 4.2. Main RTMTRACE parameters used in this work.

COMMAND SUBCOMAND	PARAMETER	
BEAM IST=4	**X0,Y0**	(X,Y) position of the particle [mm]
	XP0,YP0	divergence in (X,Y) [mm]
	E	Energy of the particle [MeV]
	P	Phase of the particle [º]
BEAM IST=5	**RS**	Rms deviation in (X,Y) (beam radius) [mm]
	RPS	Rms deviation in the divergence space (XP,YP) [mm]
	E	Reference particle energy [MeV]
	DE	Rms deviation in E [MeV]
	P	Reference particle phase [º]
	DP	Rms deviation in P [º]
	NV	Number of particles in the beam [ ]
DATAL NTYP=1	**BETA**	Cavity length
	NBET	Number of cavities with this length
	PBET	Dissipated power in each cavity walls [W]
	APER	Aperture of the accelerating structure [m]

In the present study, the process of calculation consists of the following four main steps:

(1) Adjustment of the linac to obtain the desired energy gain for a given value of β_1.

(2) Calculation of the output beam spectrum.

(3) Evaluation of the relative dose rate due to the bremsstrahlung produced by this beam.

(4) Comparison of the obtained dose rates for different values of β_1.

5) DOSE RATE STUDY

5.1) Relative dose rate

To estimate the final dose rate produced by bremsstrahlung a simplified version of the formula obtained by Okulov [20][21] was used:

$$D = K \cdot |e| \cdot E^3 \cdot N \qquad \text{(Eq. 5.1)}$$

where D [Gy] is the absorbed dose in air, due to bremsstrahlung radiation, on the axis at 1 m of the bremsstrahlung target; K is a constant which takes into account the bremsstrahlung production efficiency of the target; N is the number of electrons hitting the target and E [MeV] is the beam energy. We would like to remark that, although for the present study this will not be relevant, Okulov's formula gives the exposure, which is proportional to the absorbed dose by photons that we study. Therefore, the constant K takes also into account the conversion from exposure to absorbed dose in air (1 R = 0.00877 Gy). In case of absorption in some material this relation is different (see for example [17]).

To obtain the dose rate, the current of particles hitting the target (the output beam intensity I) must be taken into account. The formula for the dose rate becomes:

$$\dot{D} = K \cdot E^3 \cdot I \qquad \text{(Eq. 5.2)}$$

Since the dose rate is an additive quantity, in case of N particles hitting the target with different energies Eq. 5.2 takes the form:

$$\dot{D} = \sum_{i=1}^{N} K \cdot {E_i}^3 \cdot I_i = K \sum_{i=1}^{N} {E_i}^3 \cdot I_i \qquad \text{(Eq. 5.3)}$$

where E_i [MeV] is the energy of the i-th particle in the beam and I_i [A] is the current carried by this particle.

If all the electrons were of the maximal energy $E_{max} = 2.08\, MeV$ (optimal acceleration) then the produced dose rate would be:

$$\dot{D}_{max} = K \cdot {E_{max}}^3 \cdot I \qquad \text{(Eq. 5.4)}$$

Let us assume that all the N electrons which hit the target are already ultrarelativistic and each of

them carries the current $I_i = {}^{I}/_{N}$.

In the present study we will calculate the relative dose rate d:

$$d = \frac{\dot{D}}{\dot{D}_{max}} = \frac{K\sum_{i=1}^{N} {E_i}^3 \cdot I_i}{K \cdot {E_{max}}^3 \cdot I} = \frac{\frac{I}{N}\sum_{i=1}^{N} {E_i}^3}{{E_{max}}^3 \cdot I} = \frac{1}{N \cdot {E_{max}}^3}\sum_{i=1}^{N} {E_i}^3 \qquad \text{(Eq. 5.5)}$$

As one can see the value of the current and the constant *K* do not enter into the last formula and therefore will not be important for the linac optimization.

We would like to remark that the relative dose rate as defined in Eq. 5.5 does not take into account the capture efficiency of the linac

$$k = \frac{N}{N_{in}} \qquad \text{(Eq. 5.6)}$$

where N_{in} is the number of particles in the input beam.

5.2) Dependence of dose rate on energy spread

One of the objectives of this work is to relate the bremsstrahlung dose rate with output beam characteristics. With this work we demonstrate that, for a given value of the maximal energy in the beam, the dose rate grows if the output beam energy spread decreases.

Before presenting results of the numerical simulations, we are going to illustrate these concepts in a simple model of the output energy spectrum and assume it to be a step function $f(E)$ of value f_0 and width ΔE as showed in Figure 5.1.

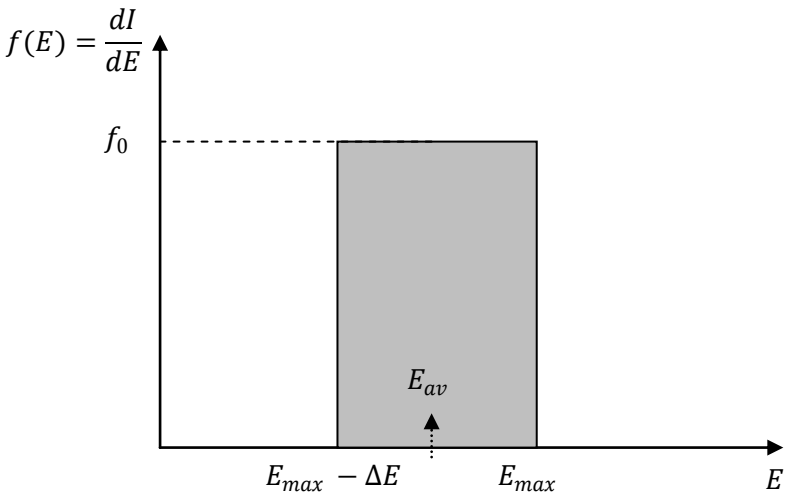

Figure 5.1. Simplified energy spectrum.

For a short interval in the spectrum Eq. 5.2 has the form:

$$d\dot{D} = K \cdot E^3 \cdot dI = K \cdot E^3 \cdot \frac{dI}{dE} \cdot dE \qquad \text{(Eq. 5.7)}$$

To obtain the dose rate we integrate along the entire energy domain:

$$\dot{D} = \int_{mc^2}^{\infty} K \cdot E^3 \cdot f(E) \cdot dE = K \cdot f_0 \int_{E_{max}-\Delta E}^{E_{max}} E^3 dE \qquad \text{(Eq. 5.8)}$$

By integrating Eq. 5.8, taking into account that, for the simplified spectrum, $I = f_0 \cdot \Delta E$ and introducing the relative width defined as $\delta = \frac{\Delta E}{E_{max}}$, we get:

$$\dot{D} = K \cdot I \cdot {E_{max}}^3 \cdot \left(1 - \frac{\delta}{2}\right) \cdot (1 - \delta + \frac{\delta^2}{2}) \qquad \text{(Eq. 5.9)}$$

To obtain the relative dose rate we should divide this last expression by the expression of the maximal dose rate from Eq. 5.4. By doing this we obtain the following analytical expression for the relative dose rate for the simplified step spectrum.

$$d = \left(1 - \frac{\delta}{2}\right) \cdot (1 - \delta + \frac{\delta^2}{2}) \qquad \text{(Eq. 5.10)}$$

Figure 5.2 shows this polynomial in the range $0 \leq \delta \leq 1$.

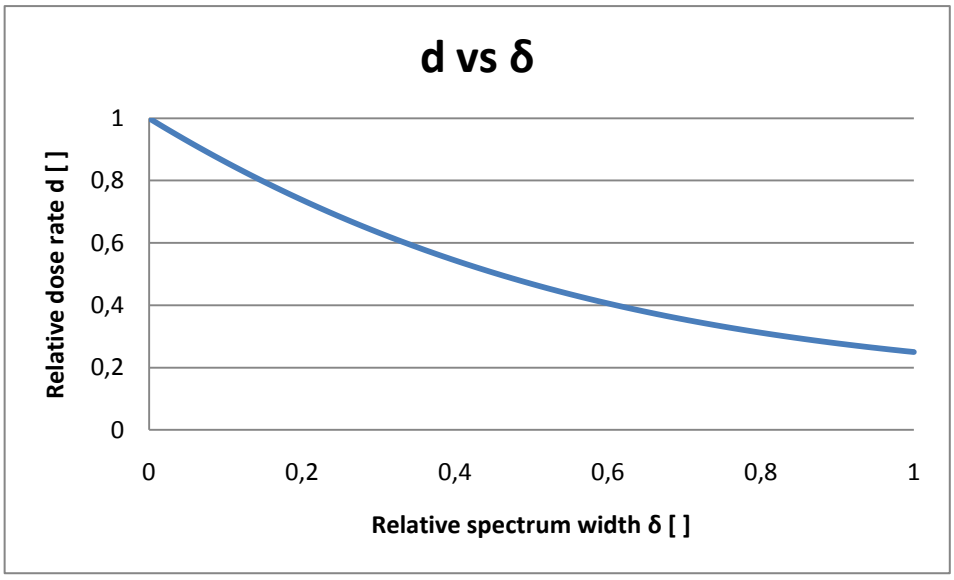

Figure 5.2. Relative dose rate d as a function of the relative spectrum width δ for the simplified spectrum.

As we can see this is a decreasing polynomial in the range $0 \leq \delta \leq 1$, meaning that the relative dose rate decreases as the spectrum width (or energy spread) increases.

For spectra with a constant maximal energy E_{max} there is a relation between the spectrum width ΔE and the average beam energy E_{av}, namely the larger is ΔE the lower is E_{av}. For our simplified model the average beam energy is:

$$E_{av} = E_{max} - \frac{\Delta E}{2} = E_{max} \cdot (1 - \frac{\delta}{2}) \qquad \text{(Eq. 5.11)}$$

and the relative width:

$$\delta = 2 \cdot (1 - \frac{E_{av}}{E_{max}}) \qquad \text{(Eq. 5.12)}$$

And we can finally, defining $\alpha = \frac{E_{av}}{E_{max}} = 1 - \frac{\delta}{2}$, express the relative dose rate d in terms of the average energy E_{av}:

$$d = \alpha \cdot (1 - 2\alpha + 2\alpha^2) \qquad \text{(Eq. 5.13)}$$

Figure 5.3 shows this polynomial in the range $0.5 \leq \alpha \leq 1$. Note that for the simple spectrum of Figure 5.1 $\alpha \geq 0.5$ always.

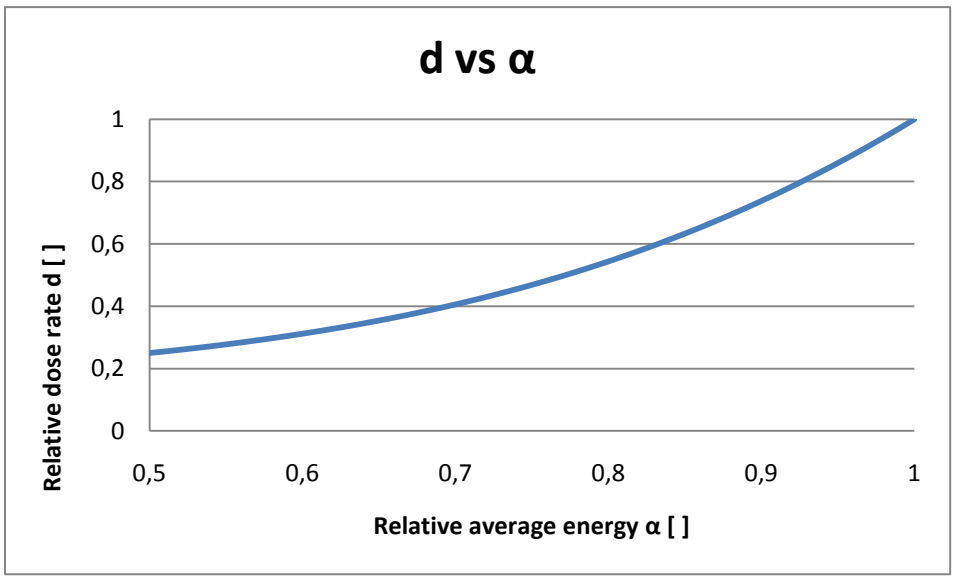

Figure 5.3. Relative dose rate d as a function of the relative average energy α for the simplied spectrum.

In the present work we will see this dependence for a more realistic beam spectrum. It will be studied numerically using the output beam characteristics and the relative dose values obtained as explained in Section 6.2.

6) NUMERICAL SIMULATION OF THE ELECTRON ACCELERATION

As it was explained in Section 4, the procedure to obtain results mainly consists of two steps:

- First, the adjustment of the linac to obtain the desired energy gain for a given value of β_1. This step is done with RTMTRACE.
- And second the calculation of the output beam energy spectrum and of the relative dose rate. This step is done with RTMTRACE and the DoseCalc code specially designed in this study.

6.1) Maximal output energy

This first step is done with the RTM simulation software RTMTRACE and the main purpose is to obtain linac configurations with the desired energy gain.

First of all we determine to which parameter is the output energy most sensitive, whether to variations of the power of the first cavity of $\beta_1<1$ (parameter P_1), or to variations of the power of the cavities of $\beta_2=1$ (parameter P_2).

A priori, we expect that the output energy is more sensitive to variations of the power P_2 because there are three cavities with this power and these cavities are longer than the first one ($\beta_2=1$). To check this in simulations with RTMTRACE, we injected individual particles with initial energy of 25 KeV and phases from -180 to 180 in three linac configurations, with β_1= 0.5, 0.7 and 0.9 respectively. For each configuration, we obtained the maximum output energy for three combinations of P_1 and P_2, one of reference, other increasing the dissipated power in the first cavity P_1 and the last increasing in the same value the dissipated power in the next three cavities P_2. Table 6.1 shows the results of this check.

Table 6.1. Results of the check of the sensitivity of the output energy.

β_1 [ ]	P_1[kW]	P_2[kW]	E_{max} [MeV]	$\Delta E_{max}/\Delta P$
0,5	150	150	1,867	-
	170	150	1,893	0,0013
	150	170	1,973	0,0053
0,7	150	150	1,99	-
	170	150	2,029	0,00195
	150	170	2,097	0,00535
0,9	150	150	1,721	-
	170	150	1,813	0,0046
	150	170	1,817	0,0048

As the table above shows, our prediction is corroborated by the results, the variation in the maximal output energy is bigger if we increase the dissipated power P_2 than if we increase P_1.

The first part of the linac optimization calculations consists of simulations of the electron acceleration. Our goal is to obtain different linac configurations, characterized by the parameters β_1, P_1 and P_2, which satisfy the condition that the desired maximum energy gain is $\Delta E = 2{,}08$ MeV. Our way to do this is:

1) Fix a value of β_1.
2) Fix a value of P_1, the power to which the output energy is less sensitive, and obtain the dependence of the output energy on the initial phase (E-PHI). From this plot we can obtain the maximal energy in the beam, and therefore the maximal energy gain.
3) By varying P_2 obtain the value which gives the desired maximal energy gain $\Delta E_{max} = 2.08 MeV$.
4) Increase the value of P_1 and repeat the steps 1) and 2). We must repeat this step to have large enough number of different linac configurations for the fixed value of β_1.
5) Change the value of β_1 and repeat all the process. We must repeat this step for all the values of β_1 chosen for the study.

Below we give an example of the input file **inp.dat** of the RTMTRACE code which calculates the dependence of the output energy on the initial phase for the case β_1=0.5, P_1=90kW, and P_2=200kW.

#INITIAL INPUT FOR DEPENDENCE OF OUTPUT ENERGY ON INITIAL PHASE #

```
BEAM  IST=4,X0=0.,XP0=0.,Y0=0.,YP0=0.,E=0.025,P=-180
BEAM  IST=4,X0=0.,XP0=0.,Y0=0.,YP0=0.,E=0.025,P=-170
                        .
                        .
                        .
BEAM  IST=4,X0=0.,XP0=0.,Y0=0.,YP0=0.,E=0.025,P=170
BEAM  IST=4,X0=0.,XP0=0.,Y0=0.,YP0=0.,E=0.025,P=180
DATA F=5712
DATL NTYP=1,BETA=0.5,NBET=1,PBET=90000.
DATL NTYP=1,BETA=1,NBET=3,PBET=200000.
DATL NTYP=1,APER=0.005, LIST=0
INTL NTYP=1,IGRA=1
PRBM
END
```

This code simulates the motion of individual particles with different phases through the linac configuration under study and displays on the screen the dependence of the output energy on the initial phase. This plot is saved in the output file **E_phi.ps** .

Figure 6.1 shows the result, from the file **E_phi.ps**, of the simulation done for the configuration β_1=0.5, P_1=90kW, and P_2=200kW.

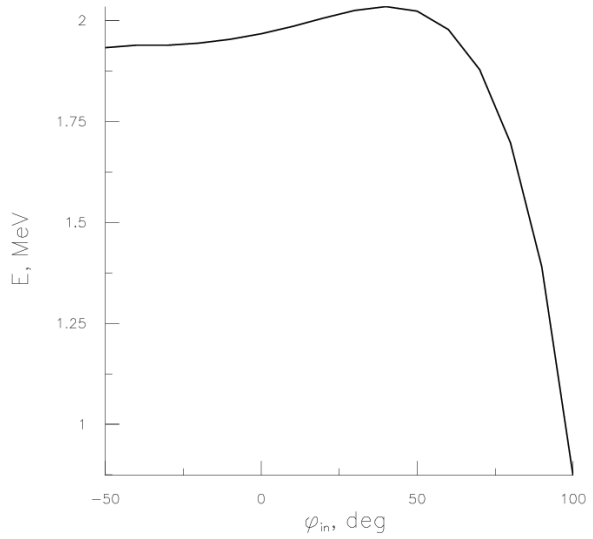

Figure 6.1. Dependence of the output energy on the initial phase for the configuration β_1=0.5, P_1=90kW, and P_2=200kW.

There are some points that one must take into account while doing this simulations:

First, the fact that in order to obtain results of a beam defined in the individual start mode (IST=4), the first particle defined (reference particle) must be captured into acceleration.

A particle must enter in the cavity at the time the field level is enough to capture it into acceleration. There is minimal phase of a particle to be captured into acceleration. Depending on the first cavity length (β_1) and its field level (given by the dissipated power in the wall P_1), the minimal phase (φ) of a particle to be captured into acceleration changes. Therefore, in the input code **inp.dat**, the phase of the reference particle must have, at least, the minimal phase φ to be captured into acceleration. In the example we have given below (configuration with BETA1=0.5, PBETA1=90kW, and PBETA2=200kW), the minimal phase to be captured into acceleration is around $\varphi = -50º$, as showed in Figure 6.1. For relativistic negative particles entering β =1 cells, particle at $+90^0$ injected phase gets maximum acceleration, because such particle passes centre of accelerating gap when the electric field is negative and its absolute value is maximum. For non-relativistic injected electrons and first cell β <1, phase of maximum acceleration depends on beam energy, β, and field strength (in Figure 6.1 it is $+50^0$).

Therefore to obtain the results of Figure 6.1, we must remove from the **inp.dat** code given bellow all particles with phase less than -50º. Thus, to obtain the minimal phase to be captured into acceleration for a given configuration, first we define a beam with phases between -180 and 180 (as in the example we have given below), and if we run the program RTMTRACE the output message is

"Linac: reference particle was lost", therefore we must increase the reference particle phase erasing the first particle definition (first line in the **inp.dat** code) and run again the program until we get results (it is not strictly necessary to erase that particle, the procedure will work also if we just move down the line in the **inp.dat,** although the plots displayed on the screen and saved in the file **E_phi.ps** are better if we erase it). Then the final input code in the example configuration, which gives as a result Figure 6.1, must be as follow.

#INITIAL INPUT FOR DEPENDENCE OF OUTPUT ENERGY ON INITIAL PHASE #

```
BEAM  IST=4,X0=0.,XP0=0.,Y0=0.,YP0=0.,E=0.025,P=-50
BEAM  IST=4,X0=0.,XP0=0.,Y0=0.,YP0=0.,E=0.025,P=-40
                        .
                        .
                        .
BEAM  IST=4,X0=0.,XP0=0.,Y0=0.,YP0=0.,E=0.025,P=170
BEAM  IST=4,X0=0.,XP0=0.,Y0=0.,YP0=0.,E=0.025,P=180
DATA F=5712
DATL NTYP=1,BETA=0.5,NBET=1,PBET=90000.
DATL NTYP=1,BETA=1,NBET=3,PBET=200000.
DATL NTYP=1,APER=0.005, LIST=0
INTL NTYP=1,IGRA=1
PRBM
END
```

Second, one must take into account that for each frequency there is a maximum in the electric field amplitude. If the electric field is over this maximum then RF discharges at the cavity internal surface with maximum field strength may appear resulting in full reflection of RF power. To take into account this RF discharge phenomenon we obtained the maximal electric field at the cavity walls for the working frequency F=5712 MHz via the Kilpatrick criterion curve (Figure 6.2) [22].

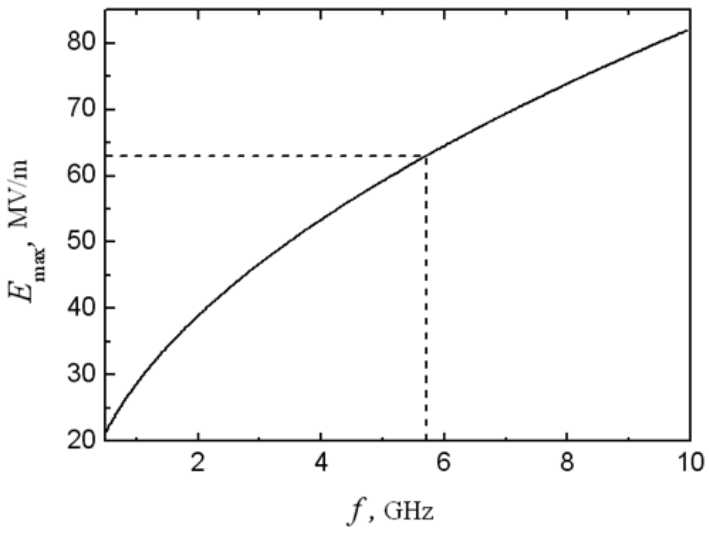

Figure 6.2. Kilpatrick criterion curve.

As one can see from the plot above the maximal electric field in the cavity walls is around $\mathcal{E}_{max}^{kp} \approx 63$ MV/m. Nowadays, with the improvement of the cavity manufacturing technologies, the Kilpatrick criterion seems to be outdated and the maximal electric field allowed in the cavity walls is several times the value obtained via the Kilpatrick criterion (depending on the material, surface quality, etc), see for example [23].

For this work we assume that the maximal electric field in the cavity wall can be 5 times the value given by the Kilpatrick criterion: $\mathcal{E}_{max}^{wall} = 5 \cdot 63 = 315\ MV/m$.

To relate the maximal electric field in the cavity walls $\mathcal{E}_{max}^{wall}$ with the maximal electric field in the cavity axis $\mathcal{E}_{max}^{axis}$ we must take into account the overstrength factor, which depends on the cavity properties.

$$k_{overstrengt\ h} = \mathcal{E}_{max}^{wall} \Big/ \mathcal{E}_{max}^{axis} \qquad \text{(Eq. 6.1)}$$

In the present work we will assume that the overstrength factor for the cavity configurations under study is of $k_{overstrengt\ h} = 4$.

Then, the maximal electric field in the cavity axis is $\mathcal{E}_{max}^{axis} = \frac{315}{4} = 79\ MV/m$.

Via RTMTRACE, we obtained the on-axis field distributions for cells with β=0.5, 0.6, 0.7, 0.8, 0.9 and 1. By increasing the dissipated power in each cavity we obtained the value of the power PBET in each cavity which gives the maximal electric field amplitude slightly less than $\mathcal{E}_{max}^{axis}$.

Bellow we give the **inp.dat** file for this part of the procedure.

```
#INPUT TO GET ELECTRIC FIELD AMPLITUDE IN THE CAVITY#
DATA F=5712.
DATL NTYP=1,BETA=0.5,NBET=1,PBET=150000.
DATL NTYP=1,APER=0.005, LIST=1
DATL NTYP=1,BETA=0.6,NBET=1,PBET=130000.
DATL NTYP=1,APER=0.005, LIST=1
DATL NTYP=1,BETA=0.7,NBET=1,PBET=170000.
DATL NTYP=1,APER=0.005, LIST=1
DATL NTYP=1,BETA=0.8,NBET=1,PBET=200000.
DATL NTYP=1,APER=0.005, LIST=1
DATL NTYP=1,BETA=0.9,NBET=1,PBET=250000.
DATL NTYP=1,APER=0.005, LIST=1
DATL NTYP=1,BETA=1.,NBET=3,PBET=270000.
DATL NTYP=1,APER=0.005, LIST=1
END
```

By running this input in RTMTRACE we obtain plots of the on-axis electric field in each cavity (saved in the file **linfield.ps**), as Figure 6.3 shows, and the file **linfield.dat** which contains information about the on-axis z-component of the electric field on the cells axis and its first derivative. By analyzing this file we obtain the maximal electric field in V/m.

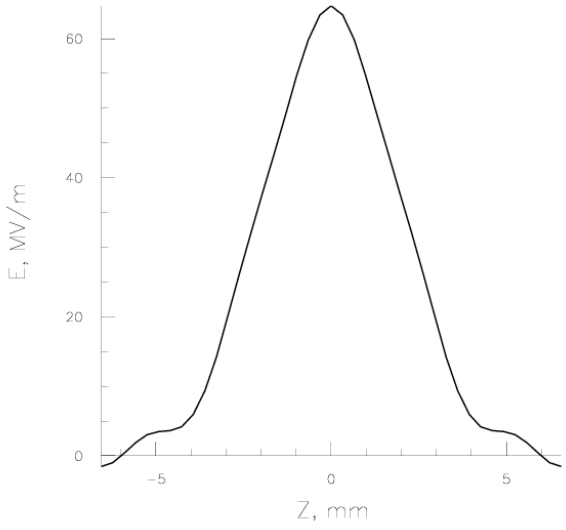

Figure 6.3. On axis electric field for a cavity with β_1=0.5 and P_1=150 kW.

Table 6.2 shows the maximal power dissipated in the cavity with the maximal electric field in the cavity walls $\mathcal{E}_{max}^{wall}$ and the maximal electric field in the cavity axis $\mathcal{E}_{max}^{axis}$ for cavities of different length.

Table 6.2. Maximal dissipated power in the cavities studied and its maximal field level at the axis and at the wall of the cell.

β [ ]	P_{max} [kW]	$\mathcal{E}_{max}^{axis}$ [MV/m]	$\mathcal{E}_{max}^{wall}$ [MV/m]
0,5	150	64,7	258,8
0,6	130	62,5	250
0,7	170	63,3	253,2
0,8	200	61,8	247,2
0,9	250	63,4	253,6
1	270	62,1	248,4

As we can see from Table 6.2, for the maximal dissipated power calculated for the cavities of different lengths, the maximal electric field in the cavity walls $\mathcal{E}_{max}^{wall}$ is less than 315 MV/m and therefore the cavities under study will not produce RF discharge in the cavity walls.

By following the procedure described above, we obtained, for each value of β_1, some pairs P_1, P_2 which give the maximal output energy of 2,08 MeV and do not produce RF discharge at the walls of the cavities.

6.2) Calculation of the output beam spectrum and the relative dose rate

At this step, the main goal is to obtain the output beam energy spectrum using the RTMTRACE code to get the relative dose rate. To do this we must simulate the dynamics of a circular beam with normal random distribution (IST=5) for the different configurations found in section 6.1, and obtain the properties of the particles of the output beam. A difficulty in doing this calculation is that the spectrum plotted by this code (command GRAF) is not precise enough, so that it is not possible to extract accurate data for the calculation of the dose rate. Figure 6.4 shows an example of the spectrum obtained with RTMTRACE. We would like to note that, in Figure 6.4, the energy relative to the energy of the reference particle in the output beam is shown and, therefore, the zero in the scale corresponds to the energy of that particle (1.93 MeV in Figure 6.4).

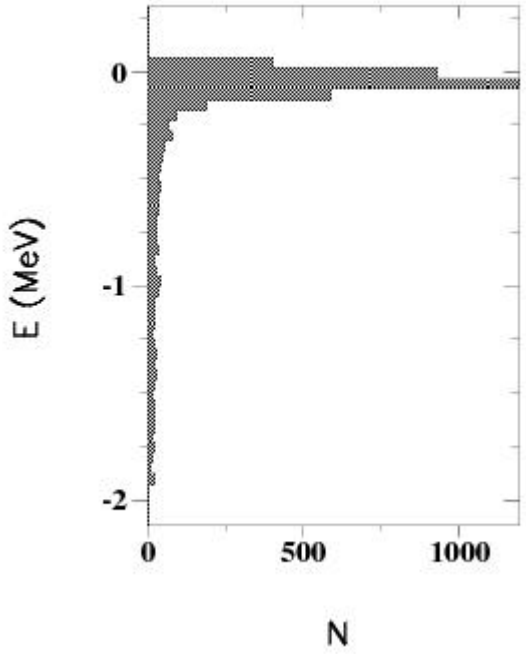

Figure 6.4. Energy spectrum obtained with RTMTRACE code using GRAF command for the configuration of β_1=0.5, P_1=100 kW and P_2=190 kW.

The method for the extraction of precise data of the output beam characteristics implemented in the present study consists in using the command DUMP to save all the properties of the particles in the output beam in the binary file **dump.dat** and then read the data of this file for further processing.

An example of the **inp.dat** file of the RTMTRACE code used to generate a file with the data of the output beam is the following:

```
#INPUT FOR OUTPUT SPECTRUM#
BEAM IST=5,RS=0.5,RPS=0.,E=0.025,DE=0.,P=0.,DP=180.,NV=10000
DATA F=5712
DATL NTYP=1,BETA=0.5,NBET=1,PBET=40000.
DATL NTYP=1,BETA=1,NBET=3,PBET=230000.
DATL NTYP=1,APER=0.005, LIST=0
INTL NTYP=1,IGRA=1
PRBM
DUMP NDMP=1
GRAF IPDE=1,IXXP=1,IYYP=1,IXY=1,IXZ=1,IYZ=1
END
```

This code simulates the behaviour in the linac of a circular beam with normal random distribution and plots the phase space projections of the output beam. All the properties of the output particles are stored in the binary file **dump.dat**.

The number of particles simulated must be sufficiently high to provide enough statistics, on one hand, and not too high so that it is possible to carry out simulations at a reasonable time, on the other hand. In this study a beam of 10000 particles was simulated.

To read and process the data of the file **dump.dat** the FORTRAN code DoseCalc was developed. DoseCalc reads a file **dump.dat** and writes the data to the file **dump.txt**, from which it can be easily extracted and processed using common software.

While doing this part of the simulations, we got some peculiar and strange results. For small values of the dissipated power in the first cavity (P_1), there turn out to be particles in the output beam with energy bigger than 2.08 MeV, although the linac configurations satisfied the condition of giving this maximal energy (as described in Section 6.1). This phenomenon is more notorious while the first cavity length (β_1) increases and most likely is related to some non-regular regimes of acceleration of off-axis particles. To get rid of such particles we had to remake, for these linac configurations, the steps explained in Section 6.1 changing the type of input beam to a more realistic beam. We changed the on-axis individual particle start (IST=4) for the circular beam with normal random distribution (IST=5) used in this section to obtain the output spectrum and the relative dose.

Once the data of the **dump.dat** file have been extracted, it is very easy to estimate the dose rate as explained in Section 5.1; these calculations have been implemented in the FORTRAN code DoseCalc which also reads the file **dump.dat**. The code is described in *Appendix A.*

7) ANALYSIS OF THE RESULTS

During the study we will use the following parameters:

a) Accelerator characteristics:

P_{tot} (kW)	- Total power in the linac.
β_1 ( )	- Beta value of the first cavity (β<1).

b) Beam acceleration characteristics (obtained from **out.dat**):

E (MeV)	- Average output beam energy.
ΔE (keV)	- Output beam energy spread.
k( )	- Capture efficiency of the configuration.

c) Bremsstrahlung dose rate characteristics (calculated with Eq. 5.5):

d ( )	- Relative dose rate.

The selection criterion implemented to choose optimal points representing a given cavity length consists in maximization of the parameter:

$$\chi = \frac{d \cdot k}{\Delta E \cdot P_{tot}} \qquad \text{(Eq 7.1)}$$

The maximization of this factor χ allows us to select combinations with a high dose rate d and capture efficiency k and with low energy spread ΔE and the dissipated power P_{tot}.

Table 7.1 shows two examples of this selection procedure.

Table 7.1. Selection of the optimal combinations for β_1=0.5 and β_1=0.9.

Case	P_{tot} [kW]	k [ ]	ΔE [keV]	d [ ]	$\chi \cdot 10^{-5}$ [$kW^{-1}keV^{-1}$]
β_1=0.5					
1	750	0,449	439,35	0,549	7,489
2	730	0,441	425,73	0,632	8,966
3	710	0,436	431,04	0,659	9,387
4	690	0,437	422,39	0,665	9,967
5	700	0,431	420,44	0,702	10,272
6	710	0,441	429,68	0,724	10,475
7	690	0,445	422,71	0,694	10,575
8	670	0,432	406,35	0,668	10,608
9	680	0,435	412,1	0,676	10,482
10	690	0,431	410,29	0,690	10,499
11	700	0,424	399,53	0,698	10,598
12	680	0,425	414,22	0,651	9,810
13	690	0,422	398,64	0,665	10,210
Selected	**670**	**0,432**	**406,35**	**0,668**	**10,608**
β_1=0.9					
1	700	0,321	407,42	0,382	4,292
2	680	0,315	471,02	0,404	3,974
3	690	0,313	467,9	0,455	4,408
4	670	0,323	477,82	0,465	4,692
5	680	0,328	476,2	0,510	5,167
6	660	0,323	495,75	0,505	4,982
7	640	0,322	496,18	0,498	5,061
8	650	0,330	496,46	0,530	5,408
9	630	0,335	506,36	0,509	5,342
10	640	0,341	516,49	0,539	5,560
11	650	0,337	511,13	0,566	5,743
12	630	0,340	505,12	0,542	5,791
13	640	0,353	514,42	0,568	6,099
14	650	0,365	507,53	0,590	6,523
15	630	0,366	500,23	0,556	6,451
Selected	**650**	**0,365**	**507,53**	**0,590**	**6,523**

Table 7.2 shows all the selected optimal configurations for each value of the first cavity length β_1 under study.

Table 7.2. Selected optimal combinations for each first cavity length β_1.

β_1 [ ]	P_{tot} [kW]	k [ ]	ΔE [keV]	d [ ]	$\chi \cdot 10^{-5}$ [$kW^{-1}keV^{-1}$]
0,5	670	0,432	406,35	0,6684	10,608
0,6	670	0,425	423,78	0,7291	10,915
0,7	650	0,427	455,79	0,7343	10,584
0,8	650	0,376	488,92	0,6988	8,268
0,9	650	0,365	507,53	0,5896	6,523

As we can see in Table 7.1 the selected configurations do not always correspond to the maximal relative dose rate among all the configurations for the same value of the first cavity length β_1. For example, in the selection of the optimal combination for $\beta_1 = 0.5$, the dissipated power in the walls and the output beam energy spread become more relevant than the relative dose rate. We can see that, for this case, the selected configuration does not give the maximal relative dose rate but the dissipated power is minimal.

7.1) Beam acceleration

In this section we summarize the results of the studies of the relation between the main accelerator characteristic and output beam parameters. In our study the accelerator characteristic is the first cavity length β_1, and the output beam parameters studied are the output beam energy E, energy spread ΔE and the capture efficiency of the accelerator k. These results characterize the efficiency of the machine.

The average output beam energy E and energy spread ΔE can be directly obtained from the file **out.dat** and the capture efficiency k is calculated from Eq. 5.6 obtaining the number of particles in the output beam N from the file **out.dat** (remember N_{in}=10000).

In Figure 7.1, 7.2, 7.5 and 7.8 different points for each value of $\beta_1$stand for configurations with different dissipated power in the cavities (P_1 and P_2). The points connected with the line (labelled as

optimal) correspond to the values which maximize the parameter χ for each value of β_1.

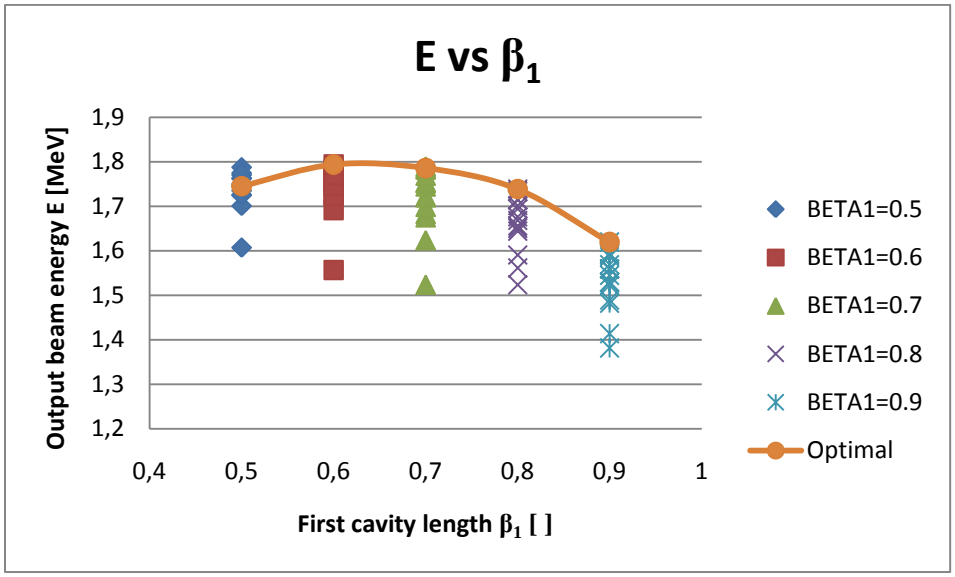

Figure 7.1. Dependence of the output beam energy E on the first cavity length β_1.

Figure 7.1 shows the plot of the average output beam energy E as a function of the first cavity length β_1. As one can see, the average beam energy E decreases, in general, while the first cavity length β_1 increases. This can be explained within the longitudinal beam dynamics. At the entrance, the initial beam is monoenergetic and continuous, this means that the particles in the input beam have the same energy E=0.025 MeV and a range of phases -180º < φ < 180º. When entering in the first cavity, some of the initial particles will be captured into acceleration (the ones which have the right phase) while others will be lost. Therefore the initial continuous beam loses its continuity and becomes a beam of bunches. For too long or too short first cell the bunch formed in the first cell will enter the second cell too late or too early leading to an ineffective acceleration and therefore a decrease of the average output beam energy.

Figure 7.2 shows the dependence of the output beam energy spread ΔE on the first cavity length β_1.

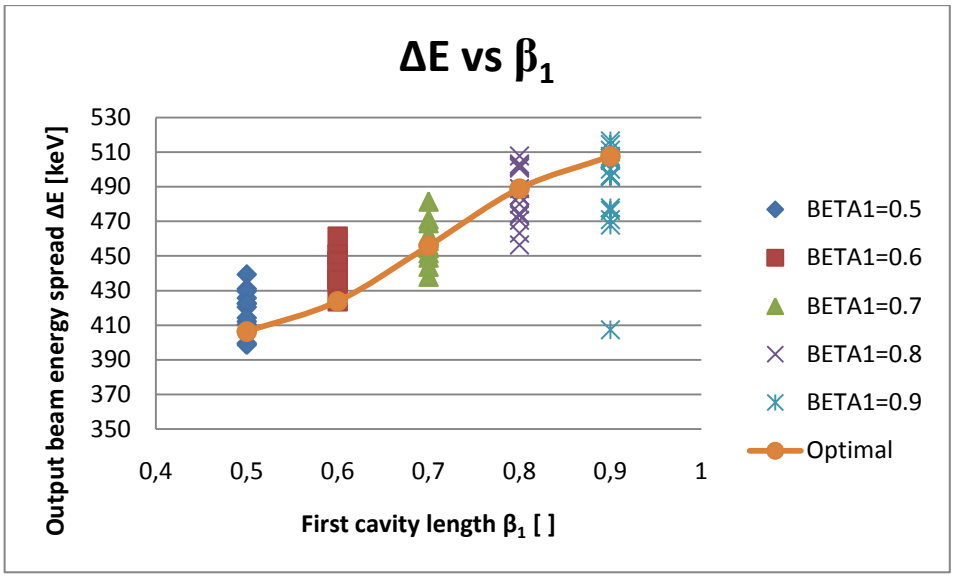

Figure 7.2. Dependence of the output beam energy spread ΔE on the first cavity length β_1.

The output beam energy spread ΔE increases with the first cavity length β_1. Due to the fact that we have set the maximal energy gain, the output beam energy spread ΔE is related to the beam energy E. If the beam energy E increases while the maximal energy gain remains constant, then the output beam energy spread ΔE must decrease. This is in qualitative agreement with Eq. 5.11.

Comparing Figure 7.1 and Figure 7.2 we can see that, for configurations of β_1>0.6, this relation is fulfilled.

For a further analysis of this dependence it is interesting to obtain plots of the output beam energy spectrum for some of the combinations of β_1, P_1, P_2 studied.

Figure 7.3 and Figure 7.4 show the output beam energy spectrum for the optimal configurations of β_1= 0.5 and β_1= 0.9 respectively.

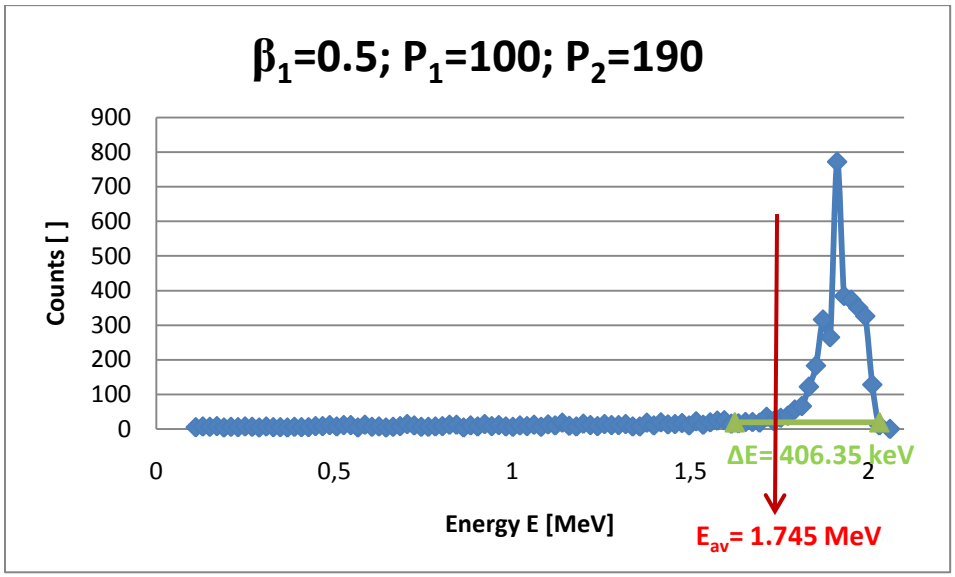

Figure 7.3. Output beam energy spectrum for the linac with β_1= 0.5, P_1=100kW and P_2= 190 kW.

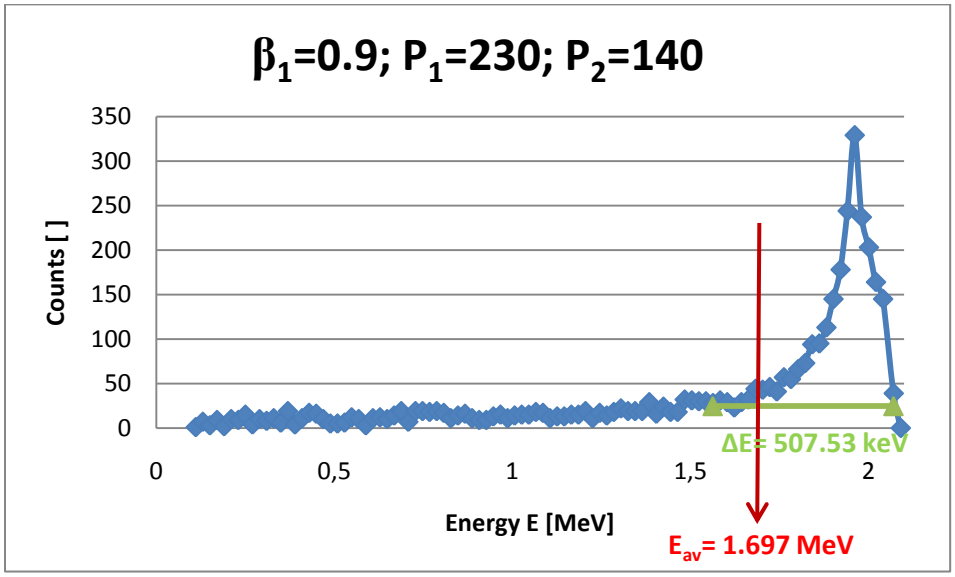

Figure 7.4. Output beam energy spectrum for the linac with β_1= 0.9, P_1=230kW and P_2= 140 kW.

If we compare the two spectra (Figure 7.3 and Figure 7.4) we can see that our qualitative conclusion above is true. While there is a slight decrease of the average beam energy E there is also a slight increase of the energy spread ΔE.

Figure 7.3 shows the relation between the capture efficiency k of the accelerator and the first cavity length β_1.

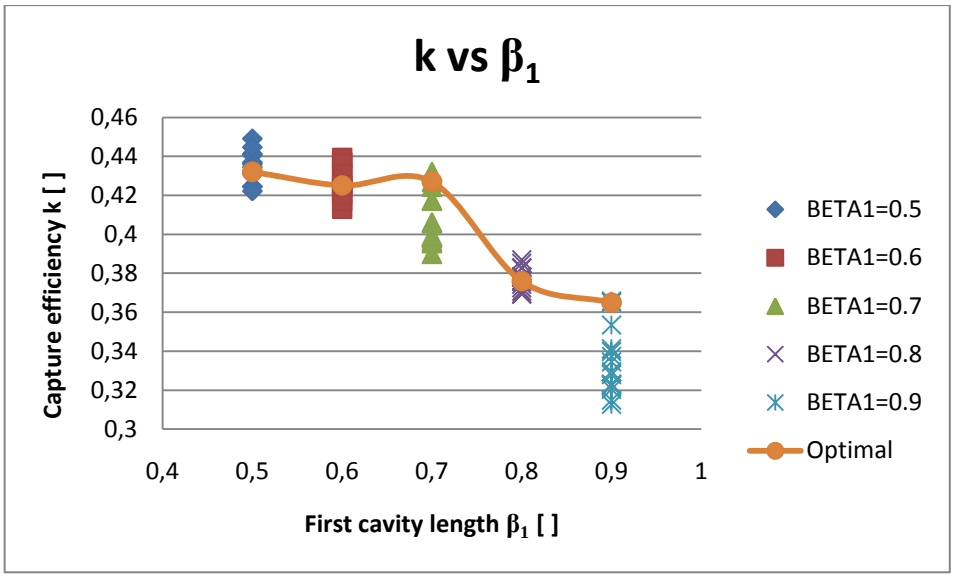

Figure 7.5. Dependence of the capture efficiency of the accelerator k on the first cavity length β_1.

As we can see from Figure 7.5, in general, k decreases as β_1 grows. For longer first cells less fraction of particles of the initial continuous beam are accelerated effectively, hence k is lower.

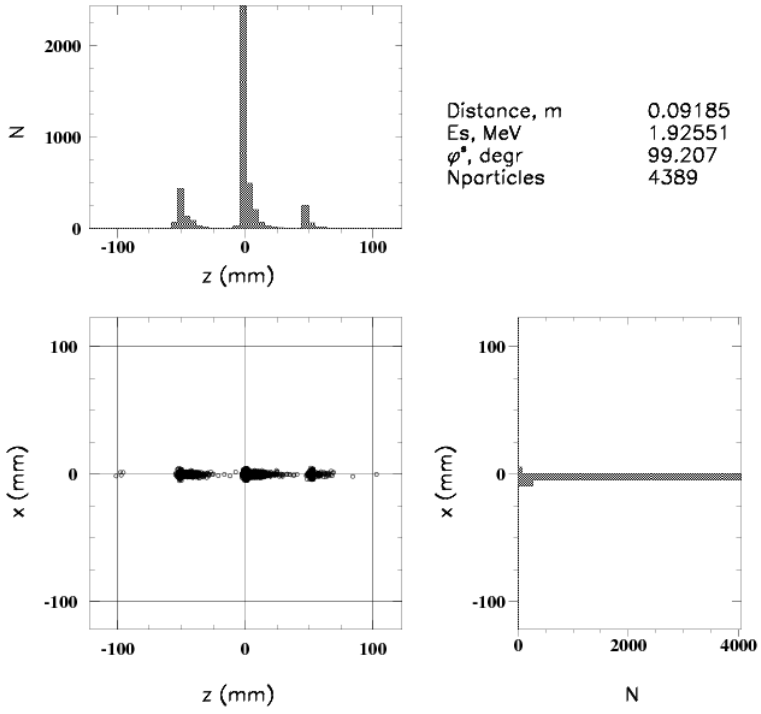

Figure 7.6. Bunching for the linac with β_1= 0.5, P_1=100kW and P_2= 190 kW.

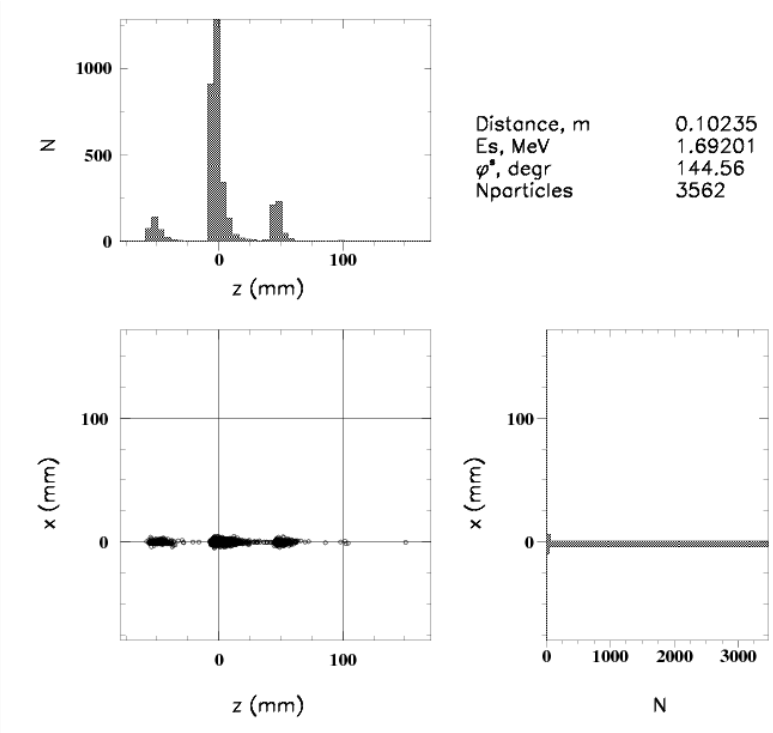

Figure 7.7. Bunching for the linac with β_1= 0.9, P_1=230kW and P_2= 140 kW.

We would like to note that though at the entrance of the linac the beam is continuous it gets bunched during the acceleration. The spatial structure of the beam at the linac exit is illustrated in Figure 7.6 and Figure 7.7. One can see that the accelerated electrons exit the linac in groups or bunches.

7.2) Dose production.

In this section we summarize the results of the study of dose production. We analyze the dependencies of the relative dose rate d on the main accelerator characteristic, the first cavity length β_1, and on the output beam parameters studied, the average output beam energy E and energy spread ΔE.

Figure 7.8 shows the relation between the relative dose rate d and the first cavity length β_1.

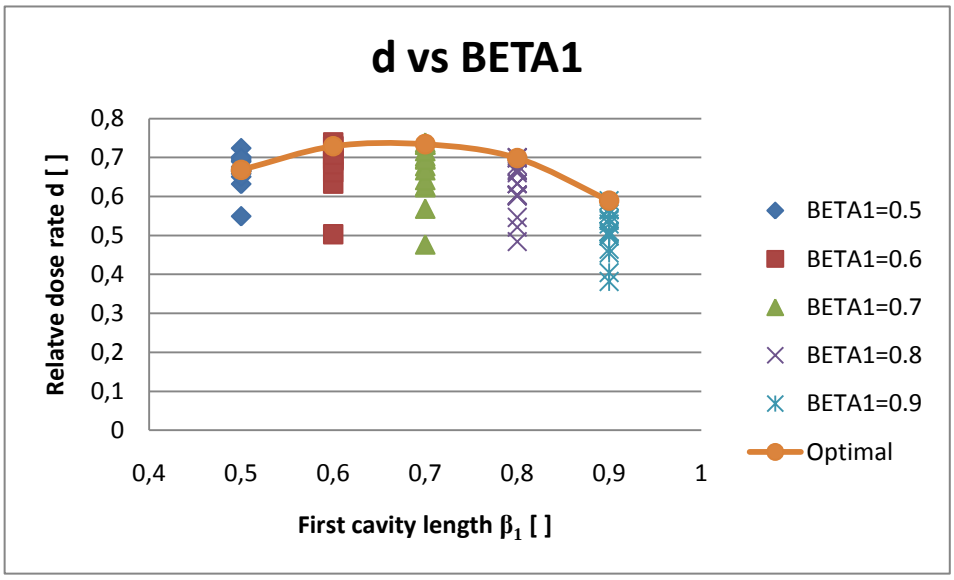

Figure 7.8. Dependence of the relative dose rate d on the first cavity length β_1.

As one can see from Figure 7.8 the relative dose rate d slightly decreases for linacs with the first cavity length β_1> 0.6. As explained in the previous section, the acceleration is less effective if β_1 is large, as a result the electrons have lower output energies and the dose rate is smaller.

Figure 7.9 and Figure 7.10 show the dependence of the relative dose rate d on the average output beam energy E and energy spread ΔE, respectively.

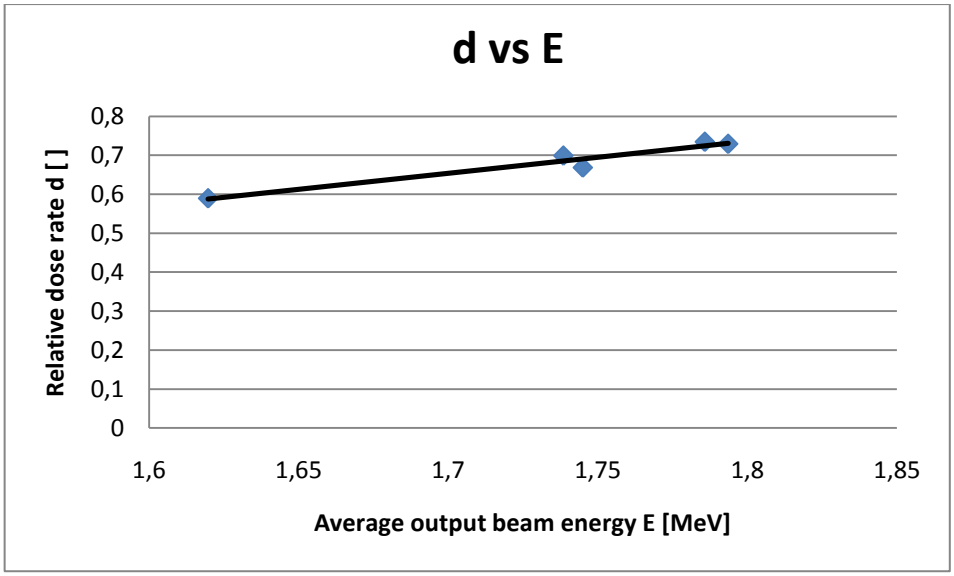

Figure 7.9. Dependence of the relative dose rate d on the average output beam energy E.

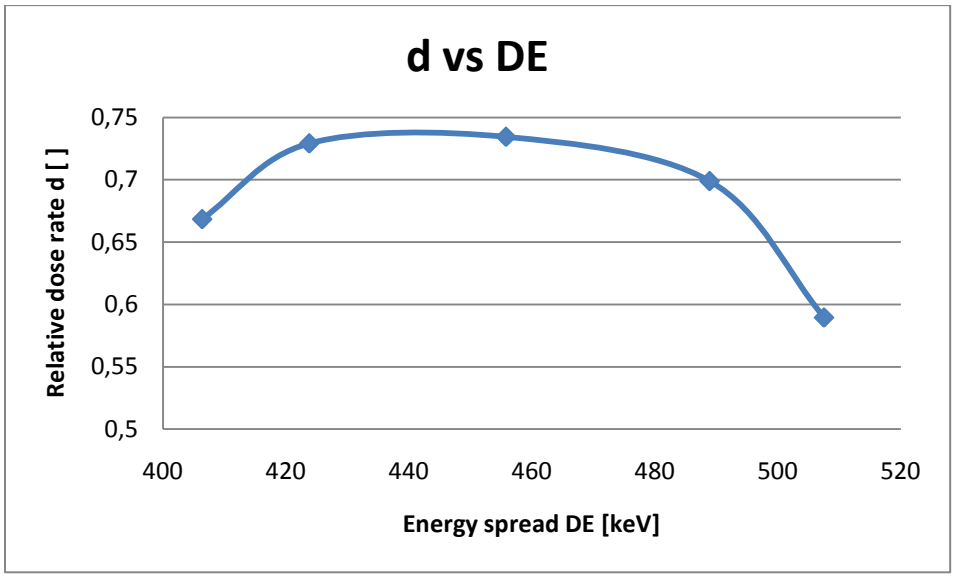

Figure 7.10. Dependence of the relative dose rate d on the output beam energy spread ΔE.

As one can see from Figure 7.9 and Figure 7.10 our result is, in general, qualitatively in agreement with the simple model of section 5.2. In Figure 7.11 and Figure 7.12 our results for the optimal configurations and those of the model, as functions of relative average beam energy α and the relative energy spread δ, respectively, are compared.

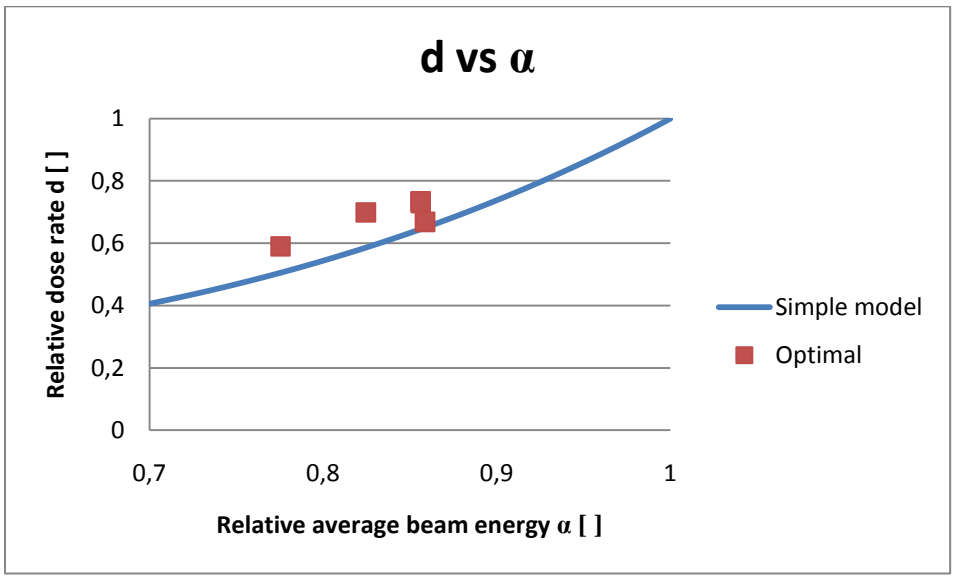

Figure 7.11. Comparison of the dependence of the relative dose rate d on the relative average beam energy α for the simple model and the realistic spectra.

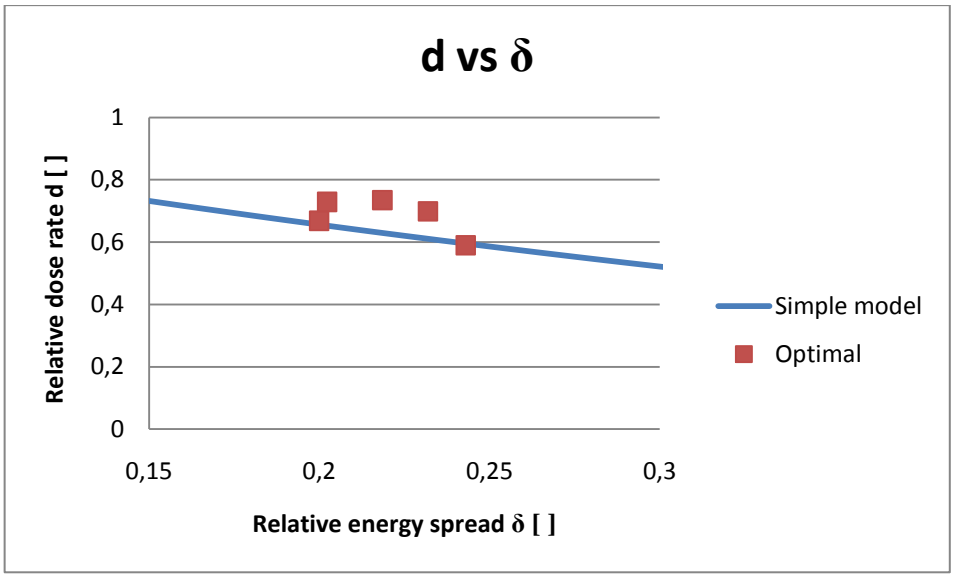

Figure 7.12. Comparison of the dependence of the relative dose rate d on the relative energy spread δ for the simple model and the realistic spectra.

As we can see from Figure 7.11 and Figure 7.12, our approximated prediction is quite accurate. The simple model prediction underestimates the relative dose rate. This is because in realistic spectra there is a long “tail” in the low energy range that, although the number of particles and its energy are low, the contribution of all them to the relative dose rate is noticeable.

8) ECONOMIC AND ENVIRONMENTAL ANALYSIS

In this section we briefly analyze the economic and environmental costs of the present work.

8.1) Economic analysis

The complete budget analysis is presented on *Appendix D*. The total project cost is 23561 €.

8.2) Environmental analysis

Due to the fact that the main part of this work is done through computer simulations, its environmental impact is very low. The amount and type of direct wastes generated in this work are the same than those from a conventional office work.

9) CONCLUSIONS

In the present work we have studied, through simulations, some aspects of the bremsstrahlung generation by linear electron accelerators related to the accelerator and its output electron beam characteristics. We studied the dose rate due to this electromagnetic radiation at fixed maximal beam energy and its dependence on the main linac parameters, such as length of the first cavity, and beam parameters, such as average energy and energy spread.

In the study we considered a simple model which relates the relative dose rate with the energy spread ΔE (and because of its relation, with the average beam energy E) of the output beam spectrum.

The simulations of the electron acceleration were done using the RTMTRACE code developed at the Skobeltsyn Institute of Nuclear Physics of Moscow State University. The procedure followed consists of four main steps:

(1) The adjustment of the linac to obtain the desired energy gain for a given value of β1: At this step we have simulated the motion of individual particles with different initial phases in the linac, and we have adjusted the dissipated power in the cavities to get the required energy gain. After this procedure we obtained, for each value of the first cavity length β_1, some pairs of dissipated powers P_1, P_2 which give the required maximal output energy of 2,08 MeV.

(2) Calculation of the output beam spectrum: To start obtaining results we simulated the motion of electrons in a circular continuous beam in the linac and obtained their properties, for different configurations studied.

(3) Evaluation of the relative dose rate due to the bremsstrahlung produced by this beam: With the properties of the output beam particles and formula taken from the literature we estimated the relative dose rate of each configuration studied.

(4) Comparison of the obtained dose rates for different values of β_1: To compare the relative dose rates obtained for the different values of the first cavity length, we selected optimal configurations with a high dose rate d and capture efficiency k and with low energy spread ΔE and total dissipated power P_{tot}.

After getting the results we analyzed relations between the studied parameters.

As we have seen in Section 7.1, there is a relation between the first cavity length β_1 and the output

beam energy spread ΔE, the output beam energy spread ΔE increases with β_1. Due to the fact that we have set the maximal energy gain, the output beam energy spread ΔE is related to the average beam energy E; and therefore there is also a relation between the first cavity length β_1 and the beam energy E, for $\beta_1 > 0.6$, the average beam energy E decreases if the first cavity length $\beta_1$increases.

In Section 7.2 we have seen that the relative dose rate d decreases for configurations with the first cavity length β_1> 0.6. We have seen also this behaviour in terms of the output beam characteristics, the relative dose rate d, in general, increases if the average output beam energy E increases and decreases if the energy spread ΔE increases. We compared the prediction of the simple model spectrum with our results and concluded that there is a qualitative agreement between them. The model however underestimates the relative dose rate.

The main conclusion of our study is that the relative dose rate of the generated bremsstrahlung radiation is maximal for the linacs with the first cavity length β_1=0.6 or β_1=0.7. Among the configurations studied, the one with $\beta_1 = 0.6$, $P_1 = 130\ kW$, $P_2 = 180\ kW$ is optimal, it gives the relative dose rate $d = 0.73$ with a capture efficiency $k = 0.4$. For linac configurations with $\beta_1 > 0.7$ both, the relative dose rate and capture efficiency, are lower.

ACKNOWLEDGEMENTS

I would like to thank Dr. Vasily Shvedunov for reading the paper and his valuable critical remarks and Dr. Yuri Koubychine for all the time and energy he has dedicated to the supervision of this project.

I would also like to thank to the *Comité de Coordinación de la Cátedra Argos* (Committee of Coordination of the Argos Professorship) for providing financial support for this work under the collaboration agreement between the *Consejo de Seguridad Nuclear* (Council of Nuclear Safety) and the *Universitat Politecnica de Catalunya* (Polytechnic University of Catalonia).

It has also been helpful the discussion with my family and friends about how to explain my ideas in a foreign language and their unconditional support during this career. Without them anything of this would happen.

REFERENCES

[1] **Haug, Eberhard.** *The Elementary process of bremsstrahlung.* New Jersey [etc.] : World Scientific, 2004

[2] **Farrell, J. Paul.** High Power Bremsstrahlung sources for radiation sterilization. *Radiation Physics and Chemistry (1977) Volume 14,* 1979, Pages 377-387.

[3] **Yu. M. Tsipenyuk.** *The Microtron: Development and Applications.* Teylor&Francis, 2002.

[4] **P. Coll.** *Fundamentos de dosimetría teórica y protección radiológica.*UPC. 1990.

[5] **Sarma, K.S.S.** Prospects and development of radiation technologies in developing countries. *Emerging applications of radiation processing.Proceedings of a technical meeting held in Vienna, April 2003.* IAEA-TECDOC-1386, January 2004. Pages 28–30.

[6] **IAEA.** *Gamma irradiators for radiation processing.* Vienna : IAEA Brochure, July 2007.

[7] **Z. Zimek.** Accelerator technology for radiation processing: recent development. *Emerging applications of radiation processing.Proceedings of a technical meeting held in Vienna, April 2003.* IAEA-TECDOC-1386, January 2004. Pages 55–63.

[8] **U. Amaldi.** The importance of particle accelerators. *Proceedings of EPAC 2000*. Pages 3-7.

[9] **R. W. Hamm.** Review of industrial accelerators and their applications. *International Topical Meeting on Nuclear Research Applications and Utilization of Accelerators*, 4-8 May 2009, Vienna

[10] **C. Tang [et al.].** Electron Linacs for cargo inspection and other industrial applications. *International Topical Meeting on Nuclear Research Applications and Utilization of Accelerators*, 4-8 May 2009, Vienna.

[11] **A.V. Poseryaev [et al.].** Design of 12 MeV RTM for multiple applications. *Proceedings of EPAC 2006*. Pages 2340-2342.

[12] **H. Wiedemann.** *Particle Accelerator Physics.(2007)*

[13] **S. Humphries, Jr.,** *Principles of Charged Particle Acceleration.*

[14] **S. Humphries, Jr.,** *Charged Particle Beams.*

[15] **K.H. Lieser,** *Nuclear and Radiochemistry: Fundamentals and Applications.* Pages 417-418.

[16] **M. G. Stabin,** *Radiation Protection and Dosimetry: an Introduction to Health Physics.* Pages 69-73.

[17] **X. Ortega, J. Jorba (Eds.).***Radiaciones ionizantes. Utilización y riesgos*. (1 y 2). Edicions UPC 1996, Barcelona. Pages 231-245

[18] **Yu.A. Kubyshin [et al.].** C-band linac optimization for a Race-Tack Microtron. *Proceedings of EPAC08.* Genoa, Italy. Pages 778-780.

[19] **V.G. Gevorkyan [et al.].** RTMTRACE, preprint VINITI 678-88 (1988).

[20] **Okulov, B.V.** *Bremsstrahlung intensity near accelerators as a function of electron energy.* 1968.

[21] **Kuznetsov, P.I.** *Dependence of bremsstrahlung dose on electron energy.* 1988.

[22] **W.D. Kilpatrick**, LBNL Report UCRL-2321 (1953).

[23] **A.Wu Chao, M. Tigner (Eds.).** *Accelerator Physics and Engineering.* World Scientific 1999.

APPENDICES

A) DoseCalc FORTRAN code

The DoseCalc FORTRAN code has been developed to read the binary file **dump.dat** generated by RTMTRACE and write the data in the file **dump.txt**. The program also gives the option to estimate the dose while extracting the data, and allows the user to customize the output beam energy spectrum (by setting the minimal and maximal values of the energy, and the number of energy discretizations) and save it in the file **spectrum.txt**.

DoseCalc works under the MS-DOS interface and only needs a **dump.dat** file (placed in the same directory of the main program) to work. The program has very simple interface and all the inputs are via the keyboard.

Once started, the program gives three options and waits for the input of a number between 1 and 3 to select each option. The options and their functions are:
Option 1: Extract dump.dat data. Extract the data stored in the binary file **dump.dat** to the formatted text file **dump.txt** without further processing.

Option 2: Plot output beam spectrum. Read the **dump.dat** file and show on the screen the maximal and minimal value of the energy in the beam and the number of particles. The program waits for the inputs of the number of divisions and the maximal and minimal values of the energy in the spectrum, then shows a very simple preview of the spectrum and gives the options to save the preview and the data table in the file **spectrum.txt**, and to remake the spectrum.

Option 3: Estimate the final relative dose. Extract the data stored in the binary file **dump.dat** in the formatted text file **dump.txt** and estimate at the same time the relative dose with the formulation given in *Section 5.1* of this work**.**

When the program has finished the chosen option, it gives the option to restart. When the program is restarted (without exiting it) the outputs in the file **dump.txt** are not erased.
Bellow we give the code of DoseCalc (comments between exclamations in cursive).

```
!PROGRAM DOSEDCALC MAIN PROGRAM!

PROGRAM DoseCalcV1
!DEFINITION OF VARIABLES!

INTEGER :: N
CHARACTER ::A
CHARACTER(LEN=50):: TitleFormat1   = "(T20,A)"
CHARACTER(LEN=50):: TitleFormat2   = "(T30,A)"
CHARACTER(LEN=50):: OptionFormat   = "(10X,A)"
!BEGINING OF THE PROGRAM!

OPEN (17,FILE='dump.txt',FORM='formatted',STATUS='unknown')
20   OPEN (15,FILE='dump.dat',FORM='unformatted',STATUS='OLD')
CALL Writetitle (6,TitleFormat1)
CALL Writetitle (17,TitleFormat2)
!PROGRAM GIVES DIFFERENT OPTIONS!
WRITE (*,OptionFormat)'1 - Extract dump.dat data'
WRITE (*,OptionFormat)'2 - Plot output beam energy spectrum'
WRITE (*,OptionFormat)'3 - Estimate the final relative dose'
WRITE (17,OptionFormat)'1 - Extract dump.dat data'
WRITE (17,OptionFormat)'2 - Plot output beam energy spectrum'
WRITE (17,OptionFormat)'3 - Estimate the final relative dose'
WRITE (*,*)
WRITE (*,OptionFormat)'Please choose one option:'
READ (*,*) N
WRITE (*,*)
WRITE (*,*)
WRITE (*,*)
WRITE (*,*)
WRITE (*,*)
WRITE (*,'(10X,A,I1)')'The option choosen was: ', N
WRITE (*,*)
```

```
      WRITE (17,*)
      WRITE (17,'(10X,A,I1)')'The option choosen was: ', N
      WRITE (17,*)
      !OPTION 1: EXTRACT DATA FROM dump.dat!
      IF (N .EQ. 1) THEN
        CALL ExtractData(15,17)
        WRITE(17,*)'dump.dat data extracted successful to dump.txt'
        WRITE(*,*)'dump.dat data extracted successful to dump.txt'
        WRITE (*,*)
        WRITE (*,*)
      !OPTION 2: PLOT SPECTRUM!
        ELSE IF (N.EQ.2) THEN
           CALL PlotSpectrum (15)
      !OPTION 3: ESTIMATE FINAL DOSE!
        ELSE IF (N.EQ.3) THEN
           CALL EstimateDose (15,17)
        ELSE IF ((N.NE.1).AND.(N.NE.2).AND.(N.NE.3)) THEN
           GOTO 20
      END IF
      WRITE (*,*)
   40 WRITE (*,*)'Do you want to restart the program(Y/N)?'
      READ (*,*)A
      WRITE (*,*)
      IF ((A.EQ.'Y').OR.(A.EQ.'y')) THEN
         WRITE (*,*)
         WRITE (*,*)
         WRITE (*,*)
         WRITE (*,*)
         WRITE (*,*)'Program restarted'
         WRITE (*,*)
         WRITE (*,*)
         WRITE (17,*)
         WRITE (17,*)
```

```
      WRITE (17,*)'Program restarted'
      WRITE (17,*)
      WRITE (17,*)
      GOTO 20
    ELSE IF ((A.EQ.'N').OR.(A.EQ.'n')) THEN
      WRITE (*,*)
      WRITE (*,*)'Program finished'
      WRITE (17,*)
      WRITE (17,*)'Program finished'
      GOTO 60
    ELSE IF (((A.NE.'Y').OR.(A.NE.'y')).AND.((A.NE.'N').OR.(A.NE.'n'))
   *)THEN
      GOTO 40
    END IF

60  CLOSE (15)
    CLOSE (17)
    END PROGRAM DoseCalcV1
                    !SUBROUTINES!

    !WRITETITLE!

    SUBROUTINE Writetitle(N, form)
    INTEGER :: N                    !in/out identificator
    CHARACTER (LEN=50) :: form      !writing format
    WRITE (N,form)  '*****************************************'
    WRITE (N,form)  '*                                       *'
    WRITE (N,form)  '*            DoseCalcV1                 *'
    WRITE (N,form)  '*                                       *'
    WRITE (N,form)  '*****************************************'
    WRITE (N,*)
    WRITE (N,*)
    WRITE (N,*)  'Universitat Politecnica de Catalunya (UPC)'
```

```
WRITE (N,*)
WRITE (N,*)
WRITE (N,*)  'Developed by:          Christian Garrido Tamm'
WRITE (N,*)  'Under the supervison of:  Prof. Youri Koubychine (Yu
*ry Kubyshin)'
WRITE(N,*)
WRITE(N,*)
WRITE (N,*)
WRITE (N,*)
END SUBROUTINE Writetitle
```

!EXTRACTDATA!

```
SUBROUTINE ExtractData (N,M)
DIMENSION X(50000),XP(50000),Y(50000),YP(50000),E(50000),
*PH(50000),NUMER(50000)
INTEGER NVEC
INTEGER ::N,M
CHARACTER(LEN=50):: LegendFormat   = "(T20,A)"
CHARACTER(LEN=50):: HeadingFormat = "(T7,A)"
CHARACTER(LEN=50):: DataFormat   = "(2I10,8(1PE12.4))"
CALL Writelegend (M,LegendFormat)
READ (N)NVEC,ISTART,Z,(X(I),XP(I),Y(I),YP(I),E(I),
*PH(I),NUMER(I),I=1,NVEC),CURR
CALL Writeheading1(M,HeadingFormat)
WRITE (M,DataFormat)NVEC,ISTART,Z,CURR
WRITE(M,*)
CALL Writeheading2 (M,HeadingFormat)
DO i=1,nvec
  WRITE (M,DataFormat)I,NUMER(I),X(I),XP(I),Y(I),YP(I),E(I),PH(I)
END DO
CLOSE(N)
END SUBROUTINE ExtractData
```

!WRITELEGEND!

```
SUBROUTINE WriteLegend(N, form)
INTEGER :: N                    !in/out identificator
CHARACTER (LEN=50) :: form          !writing format
WRITE (N,form) '-----------------------------------------------
*------------------------------'
WRITE (N,form) '| NVEC - number of particle vectors
*                    |'
WRITE (N,form) '| ISTART - type of start in BEAM command
*                    |'
WRITE (N,form) '| Z - longitudinal coordinate at which dump was do
*ne                    |'
WRITE (N,form) '| CURR - beam current
*                    |'
WRITE (N,form) '| i - Number of the particle in the dump.dat file
*                    |'
WRITE (N,form) '| Xi,XPi,Yi,YPi,Ei,PHi - 6D vector of the i-th par
*ticle                  |'
WRITE (N,form) '| Di - Dose generated due to the i-th particle
*                    |'
WRITE (N,form) '| NUMER(I) - particle number in the initial ensemb
*le, generated by BEAM command|'
WRITE (N,form) '-----------------------------------------------
*------------------------------'
WRITE (N,*)
WRITE (N,*)
WRITE (N,*)
WRITE (N,*)
END SUBROUTINE WriteLegend
```

!WRITEHEADING!

```
      SUBROUTINE Writeheading1(N, form)
      INTEGER         :: N            !in/out identificator
      CHARACTER (LEN=50):: form       !writing format
      WRITE (N,form)  'NVEC     ISTART  Z(mm)     CURR(A)'
      WRITE (N,form)  '----     ------  -----     -------'
      END SUBROUTINE Writeheading1

      SUBROUTINE Writeheading2(N, form)
      INTEGER         :: N            !in/out identificator
      CHARACTER (LEN=50):: form       !writing format
      WRITE (N,form) '   i     NUMERi   Xi(m)    XPi(rad)     Yi(m)
     *   YPi(rad)    Ei(MeV)    PHi(rad)    Di( )'
      WRITE (N,form) '  ---    -------- -------   ---------   ----------
     *  ----------  ----------  ----------  ---------'
      END SUBROUTINE Writeheading2

      !PLOTSPECTRUM!

      SUBROUTINE PlotSpectrum (N)
      DIMENSION X(50000),XP(50000),Y(50000),YP(50000),E(50000),
     *PH(50000),NUMER(50000)
      CHARACTER :: A
      INTEGER NVEC
      INTEGER ::N,Ndiv
      REAL    ::MIN,MAX
      READ (N)NVEC,ISTART,Z,(X(I),XP(I),Y(I),YP(I),E(I),PH(I),NUMER(I),
     *I=1,NVEC),CURR
   70 WRITE (*,*)'The number of particles is: ',NVEC
      WRITE (*,*)
      CALL FindMin(E,NVEC,6)
      WRITE (*,*)
      CALL FindMax (E,NVEC,6)
```

```
      WRITE (*,*)
      CALL Distribute (E,NVEC,6,MAX,MIN,Ndiv)
      WRITE (*,*)
      WRITE (*,*)
   80 WRITE (*,*)'Do you want to save this plot (Y/N)?'
      READ (*,*)A
      WRITE (*,*)
      IF ((A.EQ.'Y').OR.(A.EQ.'y')) THEN
        OPEN (19,FILE='spectrum.txt',FORM='formatted',STATUS='unknown')
        WRITE (19,'(T10,A50)')'****************************************'
        WRITE (19,'(T10,A50)')'*                                      *'
        WRITE (19,'(T10,A50)')'*   Energy spectrum:   SPECTRUM.TXT   *'
        WRITE (19,'(T10,A50)')'*                                      *'
        WRITE (19,'(T10,A50)')'****************************************'
        WRITE (19,*)
        WRITE (19,*)
        WRITE (19,'(T5,A)')'-------------------------------------'
        WRITE (19,'(T5,A)')'|                                    |'
        WRITE (19,'(T5,A,2X,I5,A)')'| The number of particles is:',NVEC
       *,' |'
        WRITE (19,'(T5,A)')'|                                    |'
        CALL FindMin(E,NVEC,19)
        WRITE (19,'(T5,A)')'|                                    |'
        CALL FindMax (E,NVEC,19)
        WRITE (19,'(T5,A)')'|                                    |'
        WRITE (19,'(T5,A,2X)')'-------------------------------------'
        CALL Distribute (E,NVEC,19,MAX,MIN,Ndiv)
        WRITE (19,*)
        WRITE (19,*)
        WRITE (*,*)'Spectrum saved in file spectrum.txt'
        WRITE (*,*)
        WRITE (17,*)'Spectrum saved in file spectrum.txt'
        WRITE (17,*)
```

```
      ELSE IF ((A.EQ.'N').OR.(A.EQ.'n')) THEN
         WRITE (*,*)'Spectrum not saved'
         WRITE (17,*)'Spectrum not saved'
         GOTO 100
      ELSE IF (((A.EQ.'Y').OR.(A.EQ.'y')).AND.((A.EQ.'N').OR.(A.EQ.'n'))
     *)THEN
         GOTO 80
      END IF
  100 WRITE (*,*)'Do you want to remake the spectrum(Y/N)?'
      WRITE (*,*)
      READ (*,*)A
      IF ((A.EQ.'Y').OR.(A.EQ.'y')) THEN
      GOTO  70
      ELSE IF ((A.EQ.'N').OR.(A.EQ.'n')) THEN
      GOTO 110
      ENDIF
      WRITE(17,*)'RESULTS IN FILE spectrum.txt'
  110 CLOSE (19)
      CLOSE (N)
      END SUBROUTINE PlotSpectrum

      !FINDMIN!

      SUBROUTINE FindMin(Array, Dim,N)
      DIMENSION Array(50000)
      INTEGER                 :: Location,Dim
      INTEGER                 :: k,N
      REAL                    :: Minimum
      Minimum  = Array(1)
      Location = 1
      DO k = 2, Dim
        IF (Array(k) < Minimum) THEN
            Minimum  = Array(k)
```

```
        Location = k
    END IF
  END DO
  IF (N.NE.6)THEN
    WRITE(N,'(T5,A,2X,I5,A)')  "| The minimum is in position ",
*Location,' |'
    WRITE(N,'(T5,A,8X,F9.8,A)')  "| Minimum value is ", Minimum,
*' |'
    ELSE
    WRITE(N,*)  "The minimum is in position ", Location
    WRITE(N,*)  "Minimum value is ", Minimum
  END IF
  END SUBROUTINE FindMin

  !FINDMAX!

  SUBROUTINE FindMax(Array, Dim, N)
  DIMENSION Array(50000)
  INTEGER                 :: Location,Dim
  INTEGER                 :: k,N
  REAL                    :: Maximum
  Maximum  = Array(1)
  Location = 1
  DO k = 2, Dim
    IF (Array(k) > Maximum) THEN
        Maximum  = Array(k)
        Location = k
    END IF
  END DO
  IF (N.NE.6)THEN
    WRITE(N,'(T5,A,2X,I5,A)')  "| The maximum is in position ",
*Location,' |'
    WRITE(N,'(T5,A,6X,F10.8,A)')  "| Maximium value is ", Maximum,
```

```
*' |'
  ELSE
  WRITE(N,*)  "The maximum is in position ", Location
  WRITE(N,*)  "Maximum value is ", Maximum
 END IF
 END SUBROUTINE FindMax

 !DISTRIBUTE!

 SUBROUTINE  Distribute(X, N, O, Max, Min, Ndiv)
 DIMENSION X(50000),Range(50000),Bucket(50000)          ! input score
 INTEGER                    :: N      ! # of scores
 INTEGER                    :: M,O, Ndiv     ! # of ranges
 INTEGER                    :: i, j
 REAL                       :: Minimum, Min, Maximum, Max,
*Step
 DO i = 1, 50000                ! clear buckets
  Bucket(i) = 0
 END DO
 IF (O.EQ.6)THEN
  WRITE(*,*)'Please enter the number of divisions'
  WRITE (*,*)'Note: the number of divisions must be acording to t
*he energy and the number of particles.'
  READ (*,*)M
  WRITE (O,*)
  WRITE (O,*)'The number of divisions is: ', M
  WRITE (*,*)
  WRITE(*,*)'Please enter the inferior limit in the histogram'
  READ (*,*)Minimum
  WRITE (O,*)
  WRITE (O,*)'The inferior limit is: ', Minimum
  WRITE (*,*)
  WRITE(*,*)'Please enter the superior limit in the histogram'
```

```
  READ (*,*)Maximum
  WRITE (O,*)
  WRITE (O,*)'The superior limit is: ', Maximum
  Max=Maximum
  Min=Minimum
  Ndiv=M
ELSE
  M=Ndiv
  Maximum=Max
  Minimum=Min
  WRITE (O,*)
  WRITE (O,*)'The number of divisions is: ', M
  WRITE (O,*)
  WRITE (O,*)'The inferior limit is: ', Minimum
  WRITE (O,*)
  WRITE (O,*)'The superior limit is: ', Maximum
END IF
DO i = 1, M                ! clear buckets
  Bucket(i) = 0
END DO
Step=(Maximum-Minimum)/M
DO i=1,(M+1)
  Range(i)=Minimum+(i-1)*Step
END DO
DO i = 1, N                ! for each input score
  DO j = 1, M              ! determine the bucket
    IF (X(i) < Range(j)) THEN
      Bucket(j) = Bucket(j) + 1
      EXIT
    END IF
  END DO                   ! don't forget the last bucket
  IF (X(i) >= Range(M))  Bucket(M+1) = Bucket(M+1)+1
END DO
```

```
CALL  Plot(Bucket, M, Range,O)          ! print a histogram
END SUBROUTINE  Distribute

!PLOT!

SUBROUTINE  Plot(Count, K, Range,N)
DIMENSION Count(50000),Range(50000),Aux(50000)
CHARACTER(LEN=50):: DataFormat1   =  '(T3,A1,F10.7,A1,F10.7,A1,6X,
*F5.0)'
CHARACTER(LEN=50):: PartA1   =  '(T2,A1,F5.3,7X,'
CHARACTER(LEN=50):: PartB1   =  '(T2,A1,F5.3,A1,F5.3,A1,'
CHARACTER(LEN=3) :: Repetition
CHARACTER(LEN=50):: Part2   =  'A,A2,F5.0)'
INTEGER         :: K,i,N

!FIND THE MAXIMUM COUNT!
Maximum  = Count(1)
DO i = 2, K
  IF (Count(i) > Maximum) THEN
      Maximum  = Count(i)
  END IF
END DO

DO i=1,K
    Aux(i)=Count(i)
END DO
!FIT THE HISTOGRAM TO SCREEN!
120   IF (Maximum >50) THEN
    Maximum = Maximum*0.5
    DO i=1,K
      Aux(i)=Aux(i)*0.5
    END DO
    GO TO 120
```

```
END IF
!PLOT FIRST LINE OF HISTOGRAM!
IF (INT(Aux(1)).NE.0)THEN
  WRITE(Repetition,'(I3)')INT(Aux(1))
  WRITE (N,*)
  WRITE(N,PartA1//Repetition//Part2) '<',Range(1), ('*', j=1,
*Aux(1)), '  ',Count(1)
  ELSE
  WRITE (N,*)
  WRITE(N,'(T2,A1,F5.3,A2,F5.0)')'<',Range(1),'  ',Count(1)
END IF
!PLOT K-2 NEXT LINES!
DO i=2,K-1
  IF (INT(Aux(i)).NE.0)THEN
  WRITE(Repetition,'(I3)')INT(Aux(i))
  WRITE (N,*)
  WRITE(N,PartB1//Repetition//Part2) '[',Range(i-1),';',Range(i)
*,')' ,('*', j=1,Aux(i)),'  ',Count(i)
  ELSE
  WRITE (N,*)
  WRITE(N,'(T2,A1,F5.3,A1,F5.3,A1,A2,F5.0)') '[',Range(i-1),
*';',Range(i),')' ,'  ',Count(i)
  ENDIF
END DO
!PLOT LAST LINE OF HISTOGRAM!
IF (INT(Aux(K)).NE.0)THEN
  WRITE(Repetition,'(I3)')INT(Aux(K))
  WRITE (N,*)
  WRITE(N,PartA1//Repetition//Part2) '<',Range(K), ('*', j=1,
*Aux(K)), '  ',Count(K)
  ELSE
  WRITE (N,*)
  WRITE(N,'(T2,A1,F5.3,A2,F5.0)')'<',Range(K),'  ',Count(K)
```

```
END IF
IF (N.NE.6)THEN
WRITE (N,*)
WRITE (N,*)
WRITE (N,"(T10,A50)")'Spectrum table:'
WRITE (N,*)
WRITE (N,'(T12,A5,15X,A6)')'Range','Counts'
WRITE (N,'(T7,15A1,8X,A10)')('-',j=1,15),'----------'
WRITE (N,*)
WRITE(N,'(T9,A1,F10.7,12X,F5.0)') '<',Range(1),Count(1)
DO i=2,K-1

  WRITE(N,DataFormat1) '[',Range(i-1),';',Range(i),')' ,Count(i)
END DO

WRITE(N,'(T9,A1,F10.7,12X,F5.0)') '>',Range(K), Count(K)
END IF
END SUBROUTINE Plot
```

!ESTIMATEDOSE!

```
SUBROUTINE EstimateDose (N,M)
DIMENSION X(50000),XP(50000),Y(50000),YP(50000),E(50000),
*PH(50000),NUMER(50000)
CHARACTER(LEN=50):: LegendFormat   = "(T20,A)"
CHARACTER(LEN=50):: HeadingFormat  = "(T7,A)"
CHARACTER(LEN=50):: ResultTitleFormat1 = "(T40,A)"
CHARACTER(LEN=50):: ResultNumberFormat1 = "(T42,F15.7)"
CHARACTER(LEN=50):: ResultTitleFormat2 = "(T25,A)"
CHARACTER(LEN=50):: ResultNumberFormat2 = "(T27,F15.7)"
CHARACTER(LEN=50):: DataFormat   = "(2I10,8(1PE12.4))"
INTEGER NVEC
INTEGER ::N
```

```
REAL::TOTALD=0,D,Emax=2.08
CALL Writelegend (17,LegendFormat)
READ (N)NVEC,ISTART,Z,(X(I),XP(I),Y(I),YP(I),E(I),
*PH(I),NUMER(I),I=1,NVEC),CURR
CALL Writeheading1(17,HeadingFormat)
WRITE (M,DataFormat)NVEC,ISTART,Z,CURR
WRITE(M,*)
CALL Writeheading2 (17,HeadingFormat)
do i=1,nvec
D= (E(I)**3)/nvec
TOTALD=TOTALD+D
WRITE (M,DataFormat)I,NUMER(I),X(I),XP(I),Y(I),YP(I),E(I),PH(I),D
end do
RELD=TOTALD/(Emax**3)
CALL WriteResult(M,ResultTitleFormat1,ResultNumberFormat1,RELD)
CALL WriteResult(6,ResultTitleFormat2,ResultNumberFormat2,RELD)
CLOSE (N)
END SUBROUTINE EstimateDose
```

!WRITERESULT!

```
SUBROUTINE WriteResult(N, form1, form2, Result)
INTEGER :: N                    !in/out identificator
CHARACTER (LEN=50):: form1, form2          !writing format
REAL :: Result
WRITE(N,*)
WRITE(N,*)
WRITE (N,form1)'THE FINAL RELATIVE DOSE IS:'
WRITE (N,form2)Result
END SUBROUTINE WriteResult
```

B) Results

B.1) Maximal output energy.

Once the procedure described in Section 6.1 is done we obtain, for each value of β_1, pairs P_1, P_2 which gives the desired energy gain as showed in next table.

β_1 [ ]	P_1 [kW]	P_2 [kW]	E_{max} [MeV]
0,5	30	240	2,0677
	40	230	2,0070
	50	220	2,0150
	60	210	2,0050
	70	210	2,0360
	80	210	2,0600
	90	200	2,0340
	100	190	2,0020
	110	190	2,0200
	120	190	2,0360
	130	190	2,0500
	140	180	2,0120
	150	180	2,0250
0,6	30	230	2,0404
	40	230	2,0943
	50	220	2,0960
	60	220	2,0809
	70	200	2,0762
	80	200	2,0650
	90	190	2,0430
	100	180	2,0150
	110	180	2,0380
	120	180	2,0580
	130	180	2,0740

(Table continues in next page)

β_1 [ ]	P_1 [kW]	P_2 [kW]	E_{max} [MeV]
0,7	40	230	2,0849
	50	220	2,0805
	60	210	2,0716
	70	200	2,0691
	80	190	2,0564
	90	190	2,0410
	100	180	2,0250
	110	180	2,0550
	120	180	2,0830
	130	170	2,0550
	140	170	2,0770
	150	160	2,0440
	160	160	2,0650
	170	160	2,0830
0,8	70	210	2,0752
	80	200	2,0829
	90	190	2,0694
	100	190	2,0931
	110	180	2,0763
	120	170	2,0696
	130	170	2,0799
	140	170	2,0300
	150	160	2,0100
	160	160	2,0400
	170	160	2,0660
	180	150	2,0370
	190	150	2,0600
	200	150	2,0810

(Table continues in next page)

β_1 [ ]	P_1 [kW]	P_2 [kW]	E_{max} [MeV]
	100	200	2,0815
	110	190	2,0480
	120	190	2,0845
	130	180	2,0662
	140	180	2,0924
	150	170	2,0707
	160	160	2,0679
0,9	170	160	2,0830
	180	150	2,0424
	190	150	2,0602
	200	150	2,0800
	210	140	2,0449
	220	140	2,0792
	230	140	2,0889
	240	130	2,0506

Table B.1. Results of linac optimization, taking into account the RF discharge effect. In grey background data obtained with IST=5.

B.2) Relative dose rate.

Once the procedure explained in Section 6.2 is done, we obtain the relative dose rate d for all the configurations from Table B.1. We can also obtain, from the output files of RTMTRACE, output beam parameters, which may be of interest, such as the number of particles, mean beam energy and energy spread.

β_1 [ ]	P_1 [kW]	P_2 [kW]	N[ ]	E [MeV]	ΔE [keV]	d [ ]
	30	240	4491	1,607	439,35	0,5495
	40	230	4407	1,701	425,73	0,6323
	50	220	4361	1,725	431,04	0,6587
	60	210	4369	1,735	422,39	0,6649
	70	210	4308	1,77	420,44	0,7018
	80	210	4413	1,788	429,68	0,7241
0,5	90	200	4447	1,762	422,71	0,6936
	100	190	4321	1,745	406,35	0,6684
	110	190	4345	1,75	412,1	0,6761
	120	190	4310	1,763	410,29	0,6896
	130	190	4244	1,775	399,53	0,6984
	140	180	4245	1,726	414,22	0,6509
	150	180	4221	1,745	398,64	0,6654
	30	230	4131	1,557	437,02	0,5033
	40	230	4172	1,692	450,74	0,633
	50	220	4259	1,727	461,22	0,7385
	60	210	4370	1,755	436,25	0,6927
	70	200	4272	1,756	434,65	0,6922
0,6	80	200	4392	1,783	450,73	0,7286
	90	190	4363	1,755	447,17	0,6963
	100	180	4237	1,724	446,33	0,6628
	110	180	4205	1,746	440,16	0,6835
	120	180	4308	1,77	436,06	0,7076
	130	180	4251	1,794	423,78	0,7291
	40	230	4063	1,524	438,12	0,4767
	50	220	3900	1,624	451,65	0,5687
	60	210	3987	1,683	449,16	0,6238
	70	200	3966	1,675		0,6268
	80	190	3989	1,699	455,12	0,6423
	90	190	3982	1,722	481,45	0,678
	100	180	3955	1,72	462,08	0,6674
0,7	110	180	3992	1,745	471,19	0,6972
	120	180	4057	1,79	454,52	0,7389
	130	170	4174	1,752	468,99	0,7031
	140	170	4270	1,786	455,79	0,7343
	150	160	4245	1,754	443,9	0,695
	160	160	4322	1,769	458,77	0,7166
	170	160	4173	1,783	461,13	0,7328

(Table continues in next page)

β_1 [ ]	P_1 [kW]	P_2 [kW]	N[ ]	E [MeV]	ΔE [keV]	d [ ]
0,8	70	210	3709	1,524	456,33	0,484
	80	200	3692	1,562	473,31	0,5214
	90	190	3759	1,591	470,6	0,5462
	100	190	3825	1,644	484,95	0,601
	110	180	3782	1,656	463,25	0,6039
	120	170	3726	1,651	474,55	0,6028
	130	170	3765	1,676	484,57	0,6327
	140	170	3779	1,714	480,01	0,6696
	150	160	3696	1,668	502,09	0,6329
	160	160	3744	1,702	500,76	0,6659
	170	160	3760	1,739	488,92	0,6988
	180	150	3869	1,694	507,71	0,6609
	190	150	3851	1,715	501,64	0,6804
	200	150	3829	1,733	503,17	0,7004
0,9	100	200	3205	1,382	407,42	0,3819
	110	190	3148	1,414	471,02	0,4044
	120	190	3127	1,482	467,9	0,4551
	130	180	3231	1,489	477,82	0,4649
	140	180	3280	1,545	476,2	0,5101
	150	170	3228	1,53	495,75	0,505
	160	160	3224	1,522	496,18	0,4984
	170	160	3295	1,559	496,46	0,5296
	180	150	3346	1,53	506,36	0,5093
	190	150	3412	1,56	516,49	0,5387
	200	150	3373	1,592	511,13	0,5657
	210	140	3398	1,569	505,12	0,5424
	220	140	3534	1,594	514,42	0,5682
	230	140	3650	1,62	507,53	0,5896
	240	130	3657	1,587	500,23	0,5559

Table B.2. Final results. In grey background data obtained with IST=5.

B.3) Energy spectra

Below we give the full data to obtain the energy spectra.

β_1=0.5 P1=100,P2=190, D=0.668		β_1=0.9 P1=230,P2=140, D=0.589	
Energy [MeV]	Counts [ ]	Energy [MeV]	Counts [ ]
0,11	5	0,11	1
0,13	7	0,13	7
0,15	6	0,15	3
0,17	8	0,17	9
0,19	4	0,19	2
0,21	6	0,21	10
0,23	5	0,23	9
0,25	7	0,25	15
0,27	6	0,27	4
0,29	4	0,29	10
0,31	7	0,31	8
0,33	5	0,33	11
0,35	5	0,35	6
0,37	4	0,37	19
0,39	6	0,39	4
0,41	5	0,41	11
0,43	5	0,43	17
0,45	8	0,45	16
0,47	8	0,47	10
0,49	11	0,49	5
0,51	7	0,51	5
0,53	11	0,53	6
0,55	11	0,55	12
0,57	4	0,57	10
0,59	12	0,59	3
0,6	6	0,61	11
0,62	7	0,63	12
0,64	4	0,65	10
0,66	6	0,67	14
0,68	8	0,69	19
0,7	14	0,71	7

(Table continues in next page)

β_1=0.5 P1=100,P2=190, D=0.668		β_1=0.9 P1=230,P2=140, D=0.589	
Energy [MeV]	Counts [ ]	Energy [MeV]	Counts [ ]
0,72	10	0,73	19
0,74	6	0,75	19
0,76	6	0,77	18
0,78	7	0,79	19
0,8	8	0,81	17
0,82	12	0,83	11
0,84	12	0,85	14
0,86	4	0,87	16
0,88	10	0,89	11
0,9	7	0,91	9
0,92	14	0,93	9
0,94	8	0,95	13
0,96	11	0,97	15
0,98	7	0,99	11
1	6	1,01	14
1,02	10	1,03	15
1,04	8	1,05	15
1,06	12	1,07	18
1,08	6	1,09	17
1,1	13	1,1	11
1,12	10	1,12	13
1,14	18	1,14	13
1,16	9	1,16	15
1,18	7	1,18	15
1,2	15	1,2	19
1,22	11	1,22	11
1,24	8	1,24	17
1,26	14	1,26	14
1,28	11	1,28	18
1,3	11	1,3	22
1,32	14	1,32	19
1,34	7	1,34	19
1,36	7	1,36	19
1,38	18	1,38	29
1,4	10	1,4	16

(Table continues in next page)

β_1=0.5		β_1=0.9	
P1=100,P2=190, D=0.668		P1=230,P2=140, D=0.589	
Energy [MeV]	Counts [ ]	Energy [MeV]	Counts [ ]
1,42	19	1,42	24
1,44	13	1,44	18
1,46	14	1,46	18
1,48	17	1,48	32
1,5	10	1,5	31
1,52	22	1,52	30
1,54	12	1,54	30
1,56	19	1,56	28
1,58	24	1,58	31
1,59	25	1,6	29
1,61	15	1,62	23
1,63	16	1,64	29
1,65	20	1,66	32
1,67	20	1,68	44
1,69	18	1,7	43
1,71	35	1,72	46
1,73	23	1,74	41
1,75	32	1,76	57
1,77	38	1,78	55
1,79	56	1,8	66
1,81	66	1,82	73
1,83	122	1,84	94
1,85	183	1,86	95
1,87	316	1,88	113
1,89	265	1,9	145
1,91	772	1,92	178
1,93	384	1,94	244
1,95	373	1,96	329
1,97	350	1,98	237
1,99	326	2	203
2,01	128	2,02	164
2,03	10	2,04	145
2,06	0	2,07	39

Table B.3. Energy spectrum tables for the optimal configurations with β_1= 0.5 and 0.9

C) Analysis of the energy spectrum width

For a further analysis of the dependence of the relative dose rate on the output beam energy spread it may be interesting to obtain plots of the output beam energy spectrum for some of the combinations of β_1, P_1, P_2 studied.

Figure C.1 and Figure C.2 show the output beam energy spectra of two different configurations with BETA1=0.5.

Figure C.3 shows the output beam spectrum of a configuration with BETA1=0.7.

Figure C.4 and Figure C.5 show the output beam energy spectra of two different configurations with BETA1=0.9.

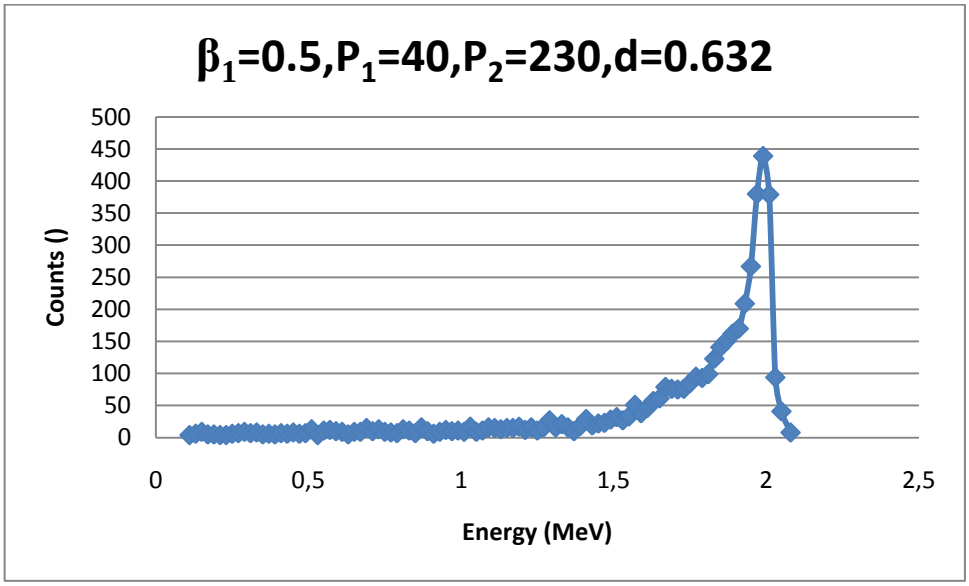

Figure C.1. Ouput beam energy spectrum for the linac with β_1= 0.5, P_1=40kW and P_2= 230 kW. The relative dose rate d in this case is 0.632.

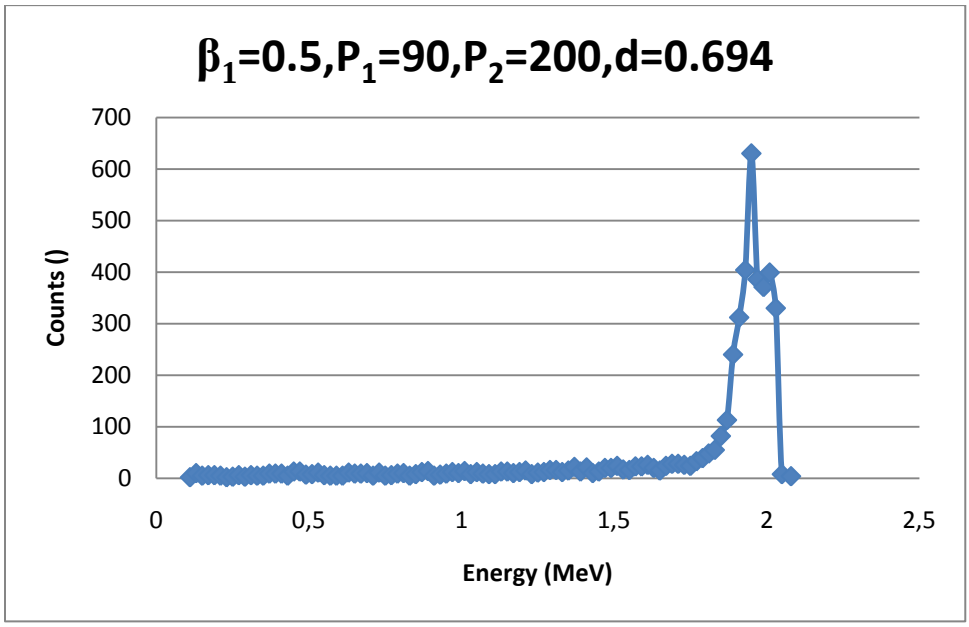

Figure C.2. Output beam energy spectrum for the linac with β_1= 0.5, P_1=90kW and P_2= 200 kW. The relative dose rate d in this case is 0.694.

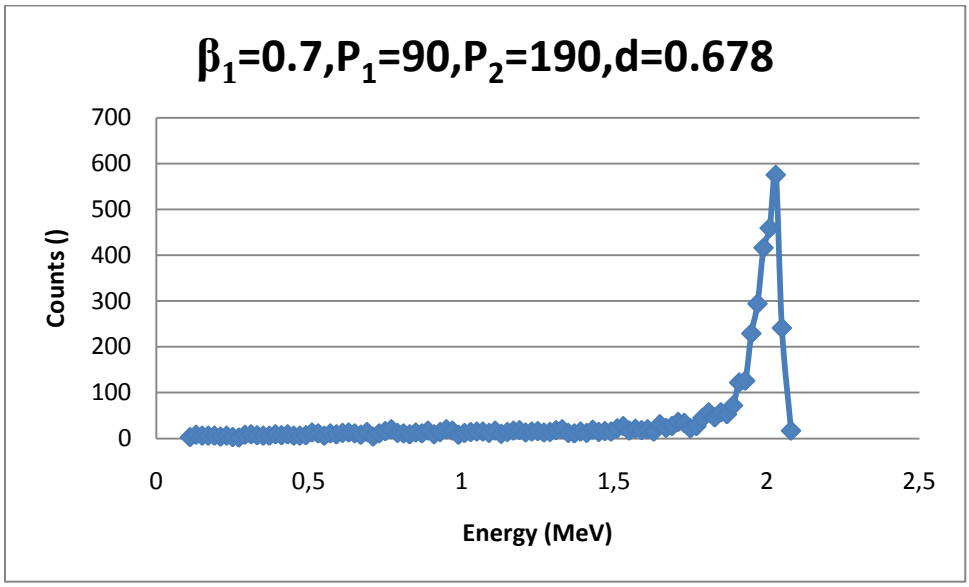

Figure C.3. Output beam energy spectrum for the linac with β_1= 0.7, P_1=90kW and P_2= 190 kW. The relative dose rate d in this case is 0.678.

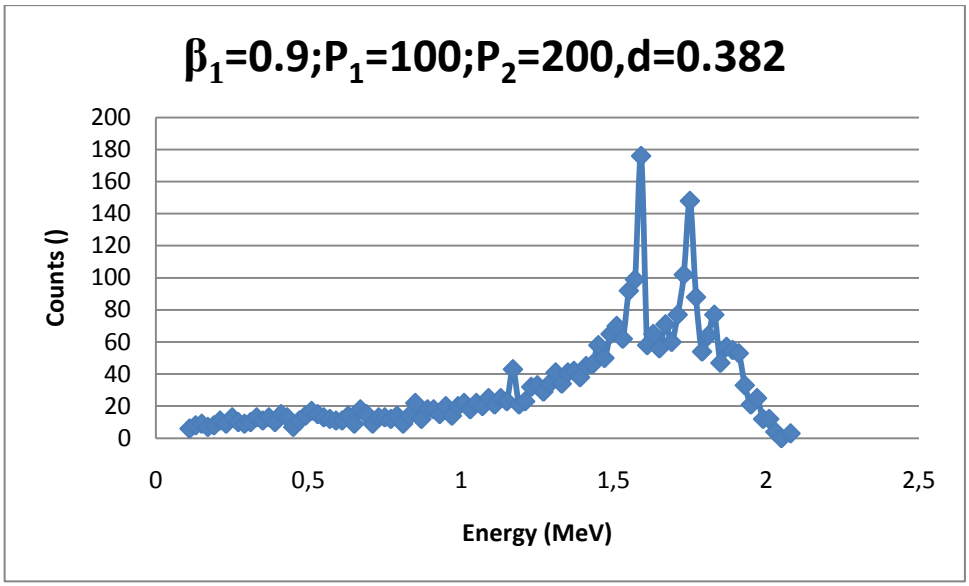

Figure C.4. Output beam energy spectrum for the linac with β_1= 0.9, P_1=100kW and P_2= 200 kW. The relative dose rate d in this case is 0.382.

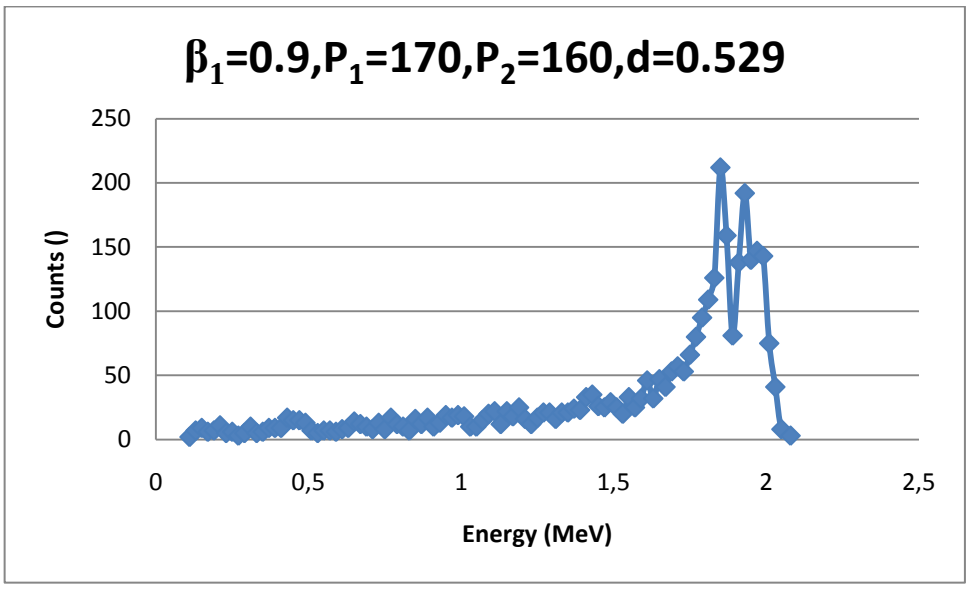

Figure C.5. Output beam energy spectrum for the linac with β_1= 0.9, P_1=170kW and P_2= 160 kW. The relative dose rate d in this case is 0.529.

To assure that the differences on the relative dose rate are not due to the long "tail" some spectra have in the low energy range we decided to study, only for two configurations, the relative dose rate due to the peak of the spectrum. The low cut-off was taken to be 1 MeV. Figure C.6 and Figure C.7 show the energy spectrum for energy higher than 1 MeV for the configurations of with β_1= 0.5, P_1=90kW and P_2= 200 kW and β_1= 0.9, P_1=100kW and P_2= 200 kW.

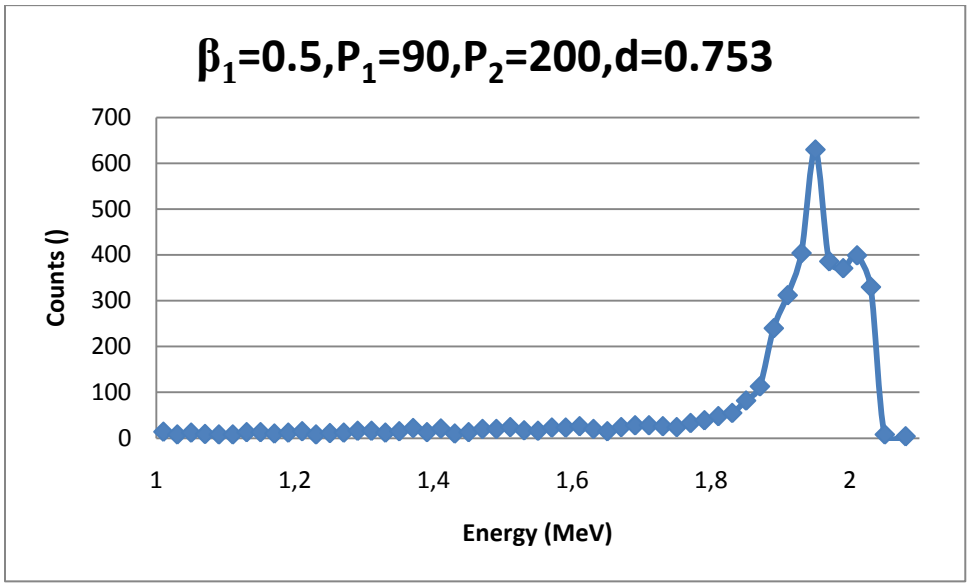

Figure C.6. Particles with energy higher than 1 MeV in the output beam for the linac with β_1= 0.5, P_1=90kW and P_2= 200 kW. The relative dose rate d due to these particles is 0.753.

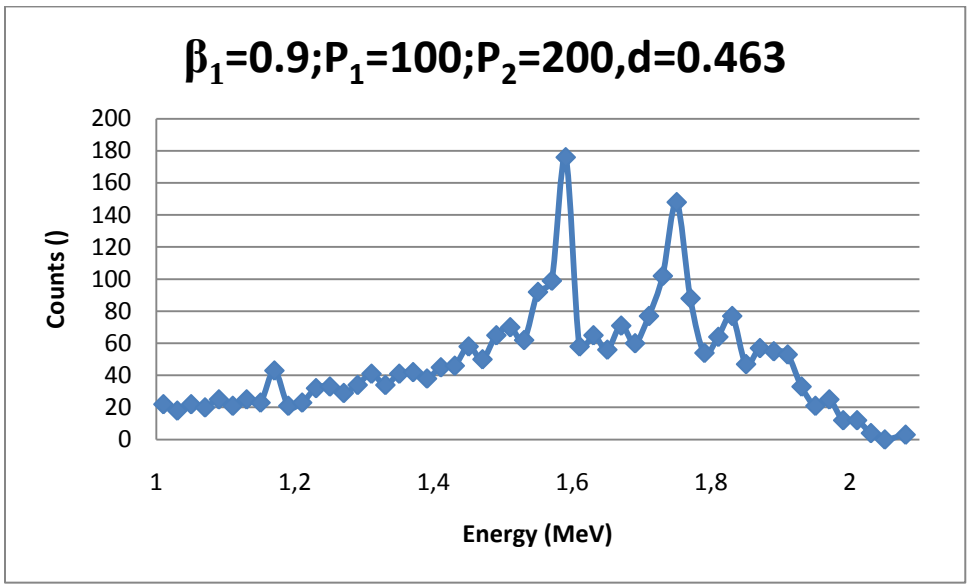

Figure C.7. Particles with energy higher than 1 MeV in the output beam for the linac with β_1= 0.9, P_1=100kW and P_2= 200 kW. The relative dose rate d due to these particles is 0.463.

Notice that, for the electrons in Figure C.6 and Figure C.7, the relative dose rate is higher than that of the whole spectrum because only particles with energies higher than 1 MeV are taken into account. If we want to see what part of the real relative dose rate (with the whole spectrum) is due to the peak we must take the number of particles to calculate the relative dose rate equal to the full number of particles in the output beam.

D) Budget

First we count the amortizable costs (to amortize in 3 years):

Concept	Cost [€]
Computer + Windows Vista operating system + Other software	1000
Printer	350
TOTAL	**1350**

This is 450 €/year of amortizable costs.

The fixed annual costs are:

- Rents, electricity, water, telephone, taxes, financial costs: 7000 €/year
- Internet connection: 360 €/year

Therefore, the total of amortizable and fixed expenses per year is:

TOTAL AMORTIZABLE AND FIXED EXPENSES PER YEAR= $\mathbf{7810}\ €/\boldsymbol{year}$

To estimate the staff costs we consider the salary of a junior engineer of 25 €/h.

Concept	Time [h]	Cost [€]
Documentation research	200	5000
Programming	80	2000
Simulations	200	5000
Analysis of results	100	2500
Memory development	200	5000
TOTAL	**780**	**19500**

Taking into account that the typical work time per year is about 1800 h/year and considering the invested time in the project about 780 h we have a total amortizable and fixed expense for project of:

TOTAL AMORTIZABLE AND FIXED EXPENSES FOR PROJECT = $\mathbf{7810}\ \frac{€}{\boldsymbol{year}} \cdot \mathbf{780}\ \boldsymbol{h} \cdot \frac{\mathbf{1}\ \boldsymbol{year}}{\mathbf{1800}\ \boldsymbol{h}} = \mathbf{3384}\ €$

If we consider a 20% error of the total cost: $3384\ € \cdot 1.2 = 4061\ €$

Therefore the total project expenses are:

TOTAL PROJECT EXPENSES= 4061 + 19500 = 23561 €